Universidade de Aveiro
2021

SUSANA MARIA VICENTE DA COSTA

OTIMIZAÇÃO DA GEOMETRIA DE UM CONVERSOR DE ENERGIA DAS ONDAS

Universidade de Aveiro
2021

SUSANA MARIA VICENTE DA COSTA

OTIMIZAÇÃO DA GEOMETRIA DE UM CONVERSOR DE ENERGIA DAS ONDAS

GEOMETRY OPTIMISATION OF A WAVE ENERGY CONVERTER

Dissertação apresentada à Universidade de Aveiro para cumprimento dos requisitos necessários à obtenção do grau de Mestre em Sistemas Energéticos Sustentáveis, realizada sob a orientação científica do Doutor Jorge Ferreira, Professor Associado do Departamento de Engenharia Mecânica da Universidade de Aveiro, e do Doutor Nelson Martins, Professor Associado do Departamento de Engenharia Mecânica da Universidade de Aveiro.

Esta dissertação teve o apoio dos projetos UIDB/00481/2020 e UIDP/00481/2020 - Fundação para a Ciência e a Tecnologia; e CENTRO-01-0145 FEDER-022083 - Programa Operacional Regional do Centro (Centro2020), através do Portugal 2020 e do Fundo Europeu de Desenvolvimento Regional.

o júri

presidente	Professora Doutora Margarita Matias Robaina professora auxiliar da Universidade de Aveiro
arguente	Doutora Vera Augusta Moreira Rodrigues investigadora doutorada (nível 1) na Universidade de Aveiro
orientador	Professor Doutor Jorge Augusto Fernandes Ferreira professor associado da Universidade de Aveiro

agradecimentos

Aos meus orientadores, Professor Jorge Ferreira e Professor Nelson Martins, por todo o acompanhamento neste trabalho, pelo apoio perante as dificuldades inerentes ao mesmo e por me motivarem a dar o meu melhor.

À minha família, por apoiarem o meu percurso académico mesmo em momentos em que tive de dedicar toda a minha atenção ao trabalho.

Ao meu namorado, João Carvalho, por todo o apoio nas vitórias e nos obstáculos, pelas críticas e sugestões, e por não me deixar esquecer a razão pela qual trabalho por ser a minha melhor versão.

Aos meus amigos, por partilharem o entusiasmo e as frustrações desta etapa final.

palavras-chave

otimização, energia das ondas, energia renovável, WEC-Sim, NEMOH, algoritmo genético.

resumo

A evolução da tecnologia e do seu acesso a nível mundial tem sido determinante no desenvolvimento de diferentes áreas científicas e de variados avanços socioeconómicos. Tanto a produção como a utilização destes equipamentos e serviços necessitam de energia, o que resultou numa escalada da sua procura e utilização e ao aumento de preocupações ambientais relacionadas com o consumo e extração de energia, havendo atualmente uma forte pressão política e social para a redução do consumo de combustíveis fósseis e, consequentemente, da sua substituição por fontes alternativas. Entre as fontes alternativas de energia, a energia renovável marinha apresenta um alto potencial, na forma de energia das ondas, das marés e térmica oceânica. No entanto, o progresso destas fontes renováveis está altamente influenciado pelo aumento do interesse e do investimento financeiro nestas tecnologias. A simulação computacional de sistemas e processos tecnológicos integrando algoritmos de otimização pode ser usada como ferramenta para reduzir o custo do desenvolvimento destas estruturas e aumentar a sua robustez, o que dará mais valor a novos projetos.

Esta dissertação visa a otimização da geometria de um conversor de energia das ondas, do tipo *point-absorber*, focando-se no aumento da absorção de energia resultante das forças de elevação. Este processo incluiu o desenvolvimento de uma geometria inicial, que foi posteriormente avaliada relativamente à sua hidrodinâmica e otimizada através de um algoritmo genético para ajustar os parâmetros da forma que influenciam a absorção de energia, com o objetivo de obter a geometria ótima. Foi definido um local de implementação, na costa portuguesa, para obter informação quanto ao tipo de onda predominante para a avaliação de diferentes estados de mar. O *software* utilizado foi o NEMOH e o WEC-Sim, ambos *open-source*, para a avaliação da interação entre a estrutura e as condições de onda impostas. Os resultados extraídos e analisados usando este *software* incluem forças nos seis graus de liberdade. Em condições de onda extremas, o maior aumento de eficiência na conversão de energia das ondas em energia mecânica entre as formas inicial e final foi de cerca de 20%, correspondendo a um aumento de 35,64% para 54,18%, enquanto em condições de mar médias, este aumento apenas atingiu o valor de cerca de 2%, correspondendo a um aumento de 22,14% para 24,51%.

keywords

optimisation, wave energy, renewable energy, WEC-Sim, NEMOH, genetic algorithm.

abstract

The evolution of technology and its worldwide access has been key in the development of different scientific areas and in several socioeconomic advances. Both production and usage of these equipment and services require energy, which resulted in the growth of its demand and use, and also led to the emergence of environmental concerns regarding energy consumption and extraction, with a current political and social pressure towards the reduction of the consumption of fossil fuels and, consequently, its substitution for alternative sources. Among the alternative energy sources, marine renewable energy presents a high potential, in the form of wave, tidal, and ocean thermal energy. The progress of these renewable sources is greatly influenced, however, by increasing interest and financial investment on these technologies. Computational simulation of technological systems and processes, integrating optimisation algorithms, may be used as a tool to reduce the cost of structure development and increase their robustness, which will add value to new projects.

This dissertation addresses the geometry optimisation of a point-absorber wave energy converter, focusing on the increase of energy absorption derived from heave forces. This process included the development of an initial geometry, which was evaluated in terms of hydrodynamics and optimised through an optimisation algorithm to tune the shape parameters that influence energy absorption with the goal of obtaining the optimal geometry. A deployment site in the Portuguese coast was defined to get information on the predominant waves for the assessment of several sea states. The used software is NEMOH and WEC-Sim, both open-source, for the evaluation of the interaction between the structure and the imposed wave conditions. The results that were extracted and analysed from this software included forces in the six degrees of freedom. Under extreme wave conditions, the highest increase in efficiency in wave energy conversion to mechanical energy between initial and final shapes was of around 20%, corresponding to an increase from 35.64% to 54.18%, while under average wave conditions, that increase only reached a value of around 2%, corresponding to an increase from 22.14% to 24.51%.

CONTENTS

LIST OF FIGURES

LIST OF TABLES

NOMENCLATURE

$\ddot{X}$	Acceleration vector of the device
λ	Wavelength [m]
ω	Wave angular frequency [rad/s]
$\overline{A(\omega)}$	Normalised radiation added mass [m^3]
$\overline{B(\omega)}$	Normalised radiation wave damping [m^3/s^2]
$\overline{C_{hs}}$	Normalised linear hydrostatic restoring coefficient [m^2]
$\overline{F_{exc}}$	Normalised wave excitation force [m^3]
ρ	Water density [kg/m^3]
$\dot{X}_{rel}$	Relative velocity of the two bodies
$A(\omega)$	Frequency dependent radiation added mass [kg]
A_{ws}	Wave spectrum coefficient
$B(\omega)$	Frequency dependent radiation wave damping [N/(m/s)]
B_{ws}	Wave spectrum coefficient
C_{hs}	Linear hydrostatic restoring coefficient [N/m]
C_{PTO}	Damping of the power take-off system [N/(m/s)]
f_p	Wave peak frequency [Hz]
f	Wave frequency [Hz]
$F_B(t)$	Net buoyancy restoring force and torque vector
$F_{exc}(t)$	Wave excitation force and torque vector
F_{exc}	Wave excitation force [N]

$F_{me}(t)$ Morison Element force and torque vector

$F_{m}(t)$ Mooring connection force and torque vector

$F_{pto}(t)$ Power take-off force and torque vector

F_{PTO} Power take-off system reaction force [N]

$F_{rad}(t)$ Wave radiation force and torque vector

F_{TH} Total heave force [N]

F_{TP} Total pitch force [N]

F_{TS} Total surge force [N]

$F_{v}(t)$ Damping force and torque vector

H_s Significant wave height [m]

H Wave height [m]

K_{PTO} Stiffness of the power take-off system [N/m]

m Body mass [kg] or Body mass matrix

P_{dens} Wave power density [kW/m]

P_{PTO} Power absorbed by the power take-off system [kW]

P_{wave} Power available in the wave for a particular device width [kW]

S_{PM} Pierson-Moskowitz spectrum [m^2/Hz]

T_p Wave peak period [s]

T Wave period [s]

X_{rel} Relative motion between the two bodies

θ Wave direction [deg]

g Gravitational acceleration [m/s^2]

BEM Boundary-Element Method

EMEC European Marine Energy Centre

PTO Power Take-Off

PM Pierson-Moskowitz

R&D Research & Development

WEC Wave Energy Converter

LCoE Levelised Cost of Energy

DOF Degrees of Freedom

1

INTRODUCTION

Western society living standards and respective supporting technology is being adopted by a growing fraction of human communities, creating a serious sustainability problem in different sectors, namely regarding energy sources [1]. From cellphones to computers, society is growing a great dependence on technological devices to operate through its many fields: health, management, engineering, among others.

All of this technology requires energy to be built, function, and be dealt with at the end of its life. Electricity is one of the main forms of energy used daily, generated through several primary sources. These include solar, wind, hydro, and fossil fuel energy. Ocean energy is at its infancy, with a long path ahead of it. This chapter has the purpose of exploring the potential of this resource, the technology around it and the tools used to optimise its components, as well as the main goals of the thesis.

1.1 FRAMEWORK

The ocean covers around 70% of the earth's surface [2] and is the supplier of many resources, ranging from biological to energetic. This energy presents itself in many forms, allowing a multitude of ways to extract and predict it. The main sources of energy in the ocean are tidal energy, ocean thermal energy, and wave energy.

Tides are generated by the interaction between the gravitational forces of the moon, the sun, and the earth. The extraction of energy from tides is not recent - it was done more than 1000 years ago in Europe to operate mills [3]. Currently, it is used to generate electricity. It is estimated that, worldwide, there is a potential for tidal energy of around 800 TWh per year, as of 2017 [4].

Ocean thermal energy is based on the temperature gradient between the top layers of the ocean, which absorb solar energy, and the deeper ones, with an optimal difference of 20 °C for most ocean thermal energy converters [3]. This source of energy is estimated to have the most potential among other marine energy sources, with a value of circa 83,300 TWh per year [3].

Lastly, there is wave energy. Waves are generated when the wind interacts with the surface of the sea, transferring the energy it has to the area of the ocean over which it acts. This energy is stored in two components: kinetic and potential, corresponding to the motion and the elevation of the water, respectively [5]. Globally, this resource is estimated to have the potential to generate 8000 - 80,000 TWh/yr [4]. In Portugal, a country bathed by the ocean, there is also an incredible amount of potential for this resource. In 2014, the value for this potential was estimated, concluding that the northern west coast of Portugal is more energetic than the southern west, with values for annual average wave energy available of 200 MWh/m and 150 MWh/m, respectively [6].

The devices used for harnessing wave energy - Wave Energy Converters (WEC) - are generally grouped according to their working principle and whether they are installed onshore or not. This classification divides the many devices in 8 main categories, as identified by the European Marine Energy Centre (EMEC) [7]. Their main features are summarised in Table 1.1, according to their working principle.

Table 1.1. Summary of the main characteristics of WECs [7].

CATEGORY	STRUCTURE	PRINCIPLE
Attenuator	Floating	Parallel to wave direction - energy harnessed from relative motion of two parts
Point Absorber	Floating	Composed by a buoyant part and a base - energy harnessed from the motion of the buoyant part relative to the base
Oscillating Wave Surge	Floating	Composed by a fixed base and an arm with free movement - energy harnessed from wave surges through the movement of the arm
Oscillating Water Column	Fixed	Structure open to the sea under the water line - energy harnessed through the changes in the air column driven by the changes in the water column inside the structure

CATEGORY	STRUCTURE	PRINCIPLE
Overtopping/ Terminator	Fixed	Structure with an upper area to store water from the break of waves - energy harnessed by the passage of that water through turbines to a lower area, returning to the sea
Submerged Pressure Differential	Fixed	Structure generally attached to the seabed - energy harnessed through the motion of the top part of the device induced by the pressure differential caused by the rise and fall of the water above it
Bulge Wave	Floating	Rubber tube filled with water moored to the seabed - energy harnessed through the passage of a 'bulge' created by the movement of water through the tube, driven by the waves
Rotating Mass	Floating	Structure with a rotating weight inside - energy harnessed through the motion of this weight caused by the passage of waves

All of these designs have summed up around 255 wave energy developers, as of the 27^{th} of August of 2020 according to EMEC [8]. The most popular category among these projects is the point absorber, rounding up 83 projects (known to the EMEC), followed by the attenuator category, with 35 projects.

However interesting and filled with potential, the wave energy sector still faces some great challenges that have been surpassed by other major renewable sources of energy, like solar and wind. Some of these challenges are related to high costs in generating energy, which leads to a disadvantage when compared to other mature technologies. Besides this, the variability and connection to the electrical grid also concern developers and investors, since the underwater cabling system must be robust and well built to integrate this energy in the mainland grid. More technically, there are problems regarding the durability of the devices at sea, where they may face tearing in chemical and physical terms, and a

technological infancy [9]. There is also an issue in conceiving a Power Take-Off (PTO) mechanism that is efficient, since there is a great variability in wave energy regarding different waves, sea states, and seasons [10]. The growing interest in wave energy has brought a lot of different types of devices, divided in the aforementioned categories, each attempting to be more economically attractive and to fix the problems that are found in earlier versions. Although this allows different designs to prosper, it also leads to a lack of a dominant system that can be considered more successful, since they are at separate levels of development and testing in open sea requires great financing and resources due to the dimensions of the devices [10].

Optimising the existing WEC systems should provide answers to many of the mentioned challenges, mainly regarding costs, performance under certain wave conditions, energy losses, among other parameters [11]. Geometry optimisation has been particularly interesting from this point of view, since most of the cost reductions can be related to the structure of the WECs [12]. Therefore, studying the shape of these devices in early stages should help solving potential structural problems before building a prototype, while also decreasing energy losses.

1.2 THESIS OBJECTIVES

Society is developing a greater independence from fossil fuels, investing in renewable energy sources both financially and in Research & Development (R&D) efforts. The ocean presents itself as a great way to achieve this goal, with a great potential to provide electrical energy to the grid. Wave energy, while still not as mature as other main renewable sources of energy, is growing as a sector in energy. This growth depends on finding the most cost competitive and efficient devices, which is heavily related to the system's design.

This thesis aims at optimising the geometry of a point-absorber WEC, specifically a heave buoy, searching for the best design in terms of structure and energy absorption, and minimising the energy losses during the harness of wave energy.

1.3 LITERATURE REVIEW

The development of diverse WECs throughout time shows the growing importance given to this resource. New designs seek to achieve cost-competitiveness with other energy sources, while also allowing a maximum of extracted energy [12].

There are several components that can be optimised to reduce costs and obtain a more efficient device. Mooring lines have been optimised in terms of maximum power, in the case of a point absorber device, in [13] using ProteusDS solver for hydrodynamic loads. They have also been optimised to reduce costs, in [14], using three different cases for the considered WECs. Both studies used surrogate-based optimisation, which seeks for a continuous function of a number of variables from available data, requiring a limited number of evaluations [15]. In cases that involve arrays of WECs, the layout of these arrays has also been subject to optimisation. Examples of these involve seeking a solution with a minimum distance between devices using a genetic algorithm [16] [17]. The influence of different device sizes within an array has also been studied using a genetic algorithm [18].

As mentioned in previous sections, geometry optimisation is a good method to reduce costs related to structure and potential energy losses. This motivated an increase in studies regarding this component of WEC design in the past few years. Geometry optimisation can be done using various procedures, which will be described in this section.

1.3.1 *Point Absorber WECs*

There are several designs and forms of wave energy converters, as presented in Table 1.1. Point absorbers are characterised by their small dimensions when compared to the wavelength of the incoming waves [19]. This property allows these devices to harness energy from any wave direction. In these systems, the relative motion of the composing parts, resulting from the interaction between the wave and the device, is used to produce power [20]. Point absorbers can be composed by one body (the motion occurs between a buoy and a fixed reference) or by two bodies (the motion occurs between a buoy and a submerged oscillating body) [21]. Several projects have been developed, with many in R&D stages and some with projected plants. As of 2013, a review made by López et al. [22] on wave energy technologies found 61 projects all over the world. This number rose to 83 in

2020, according to the EMEC [8]. An example of this system is shown in Figure 1.1, a device developed at Uppsala University in Sweden.

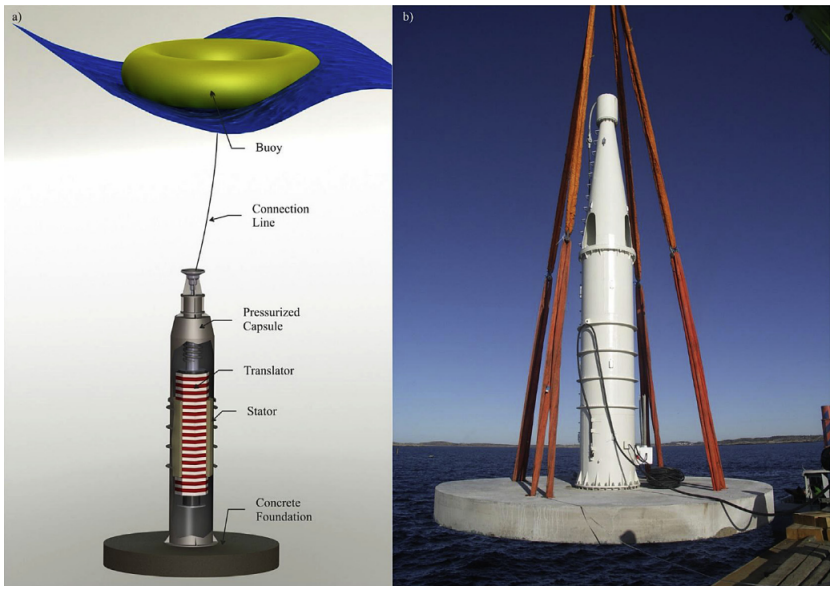

Figure 1.1. WEC device developed in Uppsala University in a) illustration and b) deployment [23].

Considering that this category is the most popular in WEC projects, there have been many studies focusing on improving the components of these devices and studying new concepts, either through numerical modelling or experimental procedures. A hybridised triboelectric-electromagnetic generator was tested in heaving point absorbers through models of the device by Saadatnia et al. [24]. This system was composed by a cylindrical freestanding grating triboelectric generator (TENG), a 3-phase tubular electromagnetic generator (EMG), and a slider (Figure 1.2). The study allowed to assess the main parameters that affected the performance of the generators.

Another concept for a point-absorber WEC was studied by Aderinto and Li [25], consisting of a self-adjustable device. It was composed of a cylindrical buoy that would slide up and down through a fixed frame, as shown in Figure 1.3, and the results showed that the annual energy was 12% higher when compared to a non-self-adjustable device.

The analysis and comparison of different designs can be done in terms of costs, which is possibly one of the most interesting variables to minimise at initial stages. In [26] a cost-based selection of design was performed on a point absorber, evaluating the Levelised Cost of Energy (LCoE) of each design in different deployment sites and with or without a fully submerged mass. This device was composed of a floating buoy and a permanent magnet linear generator, with an optional fully submerged mass connected to this generator

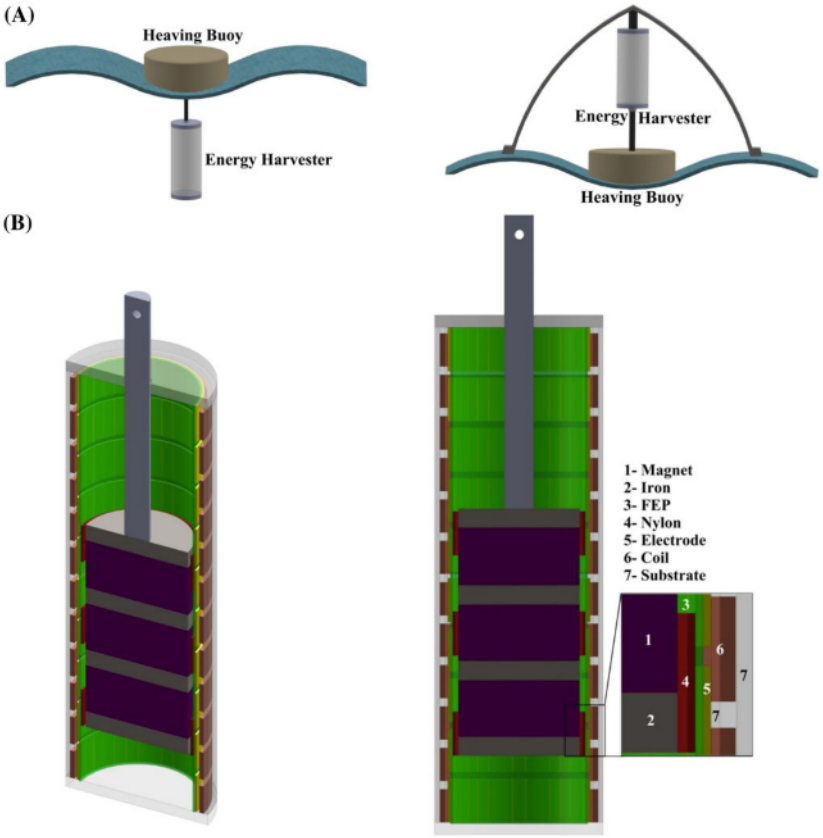

Figure 1.2. Schematics of the heaving point absorber under wave excitation (A) and configuration of the TENG and EMG generators (B) [24]

through a tensioned line. The submerged mass tunes the system's natural heave frequency according to the sea state. The results showed that the power production was greatly influenced by the deployment site and the PTO. The LCoE parameter was also affected by the submerged mass, indicating a higher LCoE without the existence of such component. Another important aspect to investigate is the survivability of the device in extreme sea states, which is demonstrated in [27]. In this study, a point absorber was tested to determine its ability to withstand loads from extreme wave conditions and the effects of these loads on the device. Several scenarios were evaluated and the results allowed to conclude that fully submerging the device when under these sea states shows more effectiveness than increasing the device's size or fixing it to the seabed. In [28] the comparison of different buoy shapes, diameters, and drafts was made using numerical models. The main two shapes that were compared were conical and hemispherical, as demonstrated in Figure 1.4. The results showed that the conical shape had a better performance than the hemispherical,

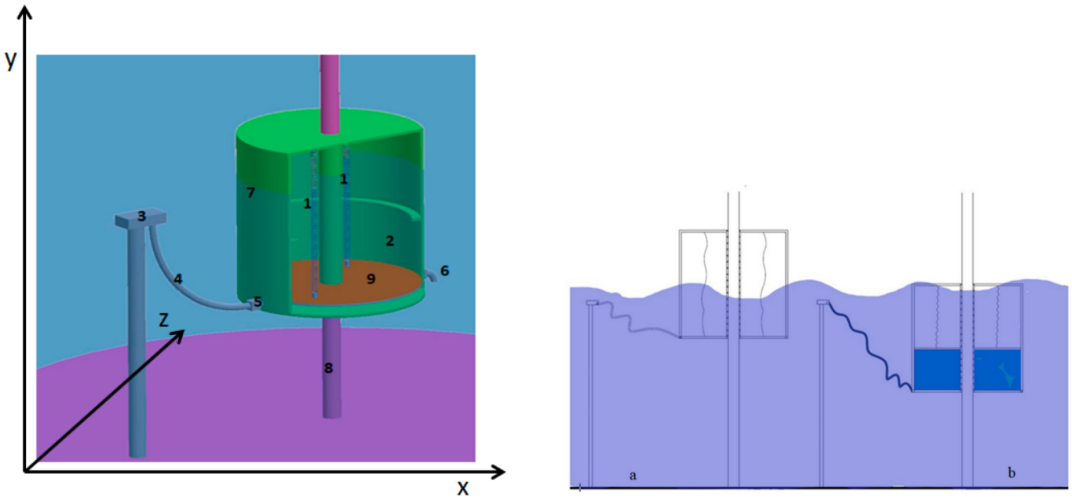

(a) Design of the point absorber.

(b) Operation stages of the device.

Figure 1.3. Self-adjustable point absorber WEC [25].

being then chosen as the focus of the rest of the study, in terms of optimal draft and diameter.

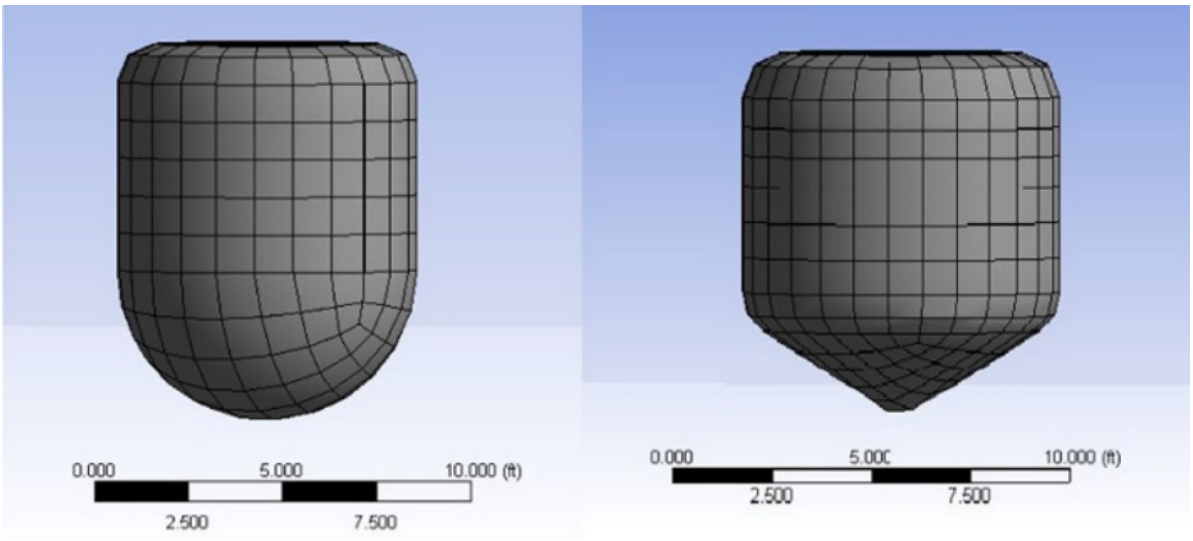

Figure 1.4. Hemispherical and conical shapes for a point absorber, respectively [28].

There are also examples of studies comparing the data provided by experimental procedures and numerical modelling, to evaluate the accuracy of the models used. Lejerskog et al. [23] performed this comparison regarding the point absorber presented in Figure 1.1 and concluded that the results were similar and that the performance of the device was influenced by the buoy's size and the translator weight. These results depend on the models developed for each device and analysis, which is related to the software

used and the theoretical assumptions. The next section aims at describing the different methods available for WEC hydrodynamic modelling.

1.3.2 *Hydrodynamic Modelling in WECs*

Studying the interaction of waves on WECs, and their behaviour in different wave conditions, may be done resorting to hydrodynamic modelling. Several software packages have been developed to be used in this context, and they differ in their approach. This difference is due to the wave theory on which the used models are based - linear or nonlinear. Penalba et al. [29] suggests that there should be three levels of linearity when assessing WECs, since linear models overestimate power production and may lead to inaccuracies in the reproduction of the WEC behaviour, as represented in Figure 1.5.

The different operating modes shown depend on the sea state. Power production mode is activated when the device is able to produce power without being compromised structurally, and survival mode is activated during extreme conditions to ensure the device's integrity. As the sea conditions worsen in terms of energy, nonlinear approaches are chosen to reproduce the WEC behaviour.

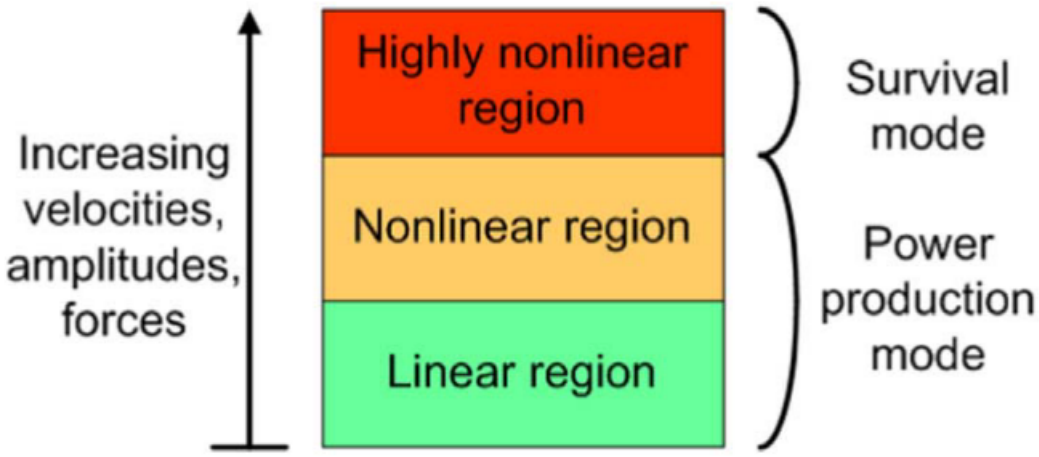

Figure 1.5. Operating regions for WECs in terms of linearity [29]

However, Wendt et al. [30] compared the results from using linear, weakly nonlinear, and fully nonlinear models in WECs and concluded that there is no relevant difference between each of them in small and medium wave conditions, sparing the cost and computational effort of using nonlinear models. Considering these recent results, the following review will include models based on linear wave theory for WECs.

In the recent years, more attention has been given to the analysis and optimisation of WECs and to the different methods involved in these processes. This interest leads to the comparison of different approaches and their advantages. NEMOH is an open-source Boundary-Element Method (BEM) code used to calculate several hydrodynamic coefficients [31], similarly to WAMIT, which uses the boundary integral equation method as its solver to obtain the relevant hydrodynamic parameters, although it requires a paid license [32]. In 2017, Penalba et al. [29] compared the usage of software WAMIT and NEMOH for wave energy studies, and concluded that NEMOH is much more user-friendly than WAMIT, specially for new users who have little experience in this subject, turning it into an easier tool to use in wave energy studies. NEMOH is also used in 2017 by Abdelkhalik et al. [33] to optimise the geometry of a heaving axisymmetric single-body device, obtaining results at different computational efforts for three test cases. One particular conclusion to take from this study is that some shapes may be discarded because NEMOH could not provide accurate results for them due to their complexity. In 2019, Alamian et al. [34] performed a multi-objective optimisation on a pitch point absorber using NEMOH, evaluating three geometry sections. The study allowed to conclude that WEC oscillations increase with the decrease of its length. Thomsen et al. [14] performed a cost optimisation of the mooring system of a floating WEC, using NEMOH to obtain hydrodynamic parameters such as added mass, radiation damping, and wave excitation, resulting in four different solution cases. Arrays of WECs have also been modelled in the frequency-domain by Wei et al. [35], calculating hydrodynamic coefficients through NEMOH. The results allowed to verify an anti-resonant behaviour of this particular configuration, which could lead to a destructive effect on energy extraction. Concerning the shape of WECs, Esmaeilzadeh and Alam [36] performed an optimisation process for different wave directions. In this case, NEMOH was also used to calculate the hydrodynamic coefficients, but there was also an analytical solution for comparison.

WAMIT has also been widely used as a solver in WEC optimisation and analysis. McCabe et al. [37] optimised the shape of a surge-and-pitch WEC using WAMIT, and obtained results for the best cost function shapes out of 180 runs of the optimisation algorithm. Sjokvist et al. [38] studied the optimisation of point absorbers, combining parameters such as radius of the buoy, cost, and damping. The study concludes that in terms of cost, a lower radius would be preferable, however, in terms of damping, the system would benefit from a higher radius, which ended up being the best solution. Falcao et al. [39] evaluated the performance

of an oscillating water column spar buoy WEC, using WAMIT as a tool to calculate the added mass and the radiation damping coefficient. A hinged type WEC was analysed and optimised by Li et al. [40], after a small scaled model had been tested in a wave basin. The vertical hinge motion was calculated in several wave periods recurring to WAMIT. Van Rij et al. [41] developed an estimation method for design loads on WECs using WAMIT to analyse a case study in terms of hydrodynamics and generalised body-modes.

Another used software is ANSYS's module AQWA, which may provide results of hydrodynamics diffraction analysis. Shadman et al. [20] performed an optimisation study on a one-body heaving point-absorber using ANSYS-AQWA to obtain results from a hydrodynamic diffraction analysis. The optimisation was based on statistical analysis methods. It is also possible to evaluate the performance of WECs, with [42] as an example. In this particular study, a new concept of wave energy converter was considered and ANSYS-AQWA used to assess the WEC's performance under regular wave conditions. Dong et al. [43] carried out a numerical study on a raft WEC, along with a structural optimisation, using AQWA as a tool for the numerical simulation. Seven structural parameters were considered and, among other conclusions, the study allowed to conclude that the length and cross-section of a single float can be defined considering the sea state. The authors suggest using the resonance phenomenon to achieve the best values. Ji [44] modelled linear and non-linear two-body WECs under both regular and irregular wave conditions, using AQWA to obtain hydrodynamic parameters. The conclusions included the great influence of PTO stiffness coefficient and submerged body geometry on power output in regular waves. A pitching float wave energy converter was analysed by Ma et al. [45] regarding its hydrodynamic performance, and AQWA was used to perform this analysis in the frequency and time domains.

WEC-Sim, a different software for hydrodynamic modelling, was also used by Van Rijn et al. [41] in the case study of estimation of design loads on WECs, providing a second set of design loads, besides the one provided by WAMIT, but this one in the time-domain. Chandrasekaran and Sricharan [46] analysed a new concept for a floating WEC with five different float configurations with numerical simulations in the frequency and time domains using WEC-Sim. A study conducted by Pardonner et al. [47] focused on a new design for an attenuator WEC combined with modules of variable geometry, and developed a numerical model for this concept using WEC-Sim to study its performance.

ANSYS-Fluent presents another great solution for hydrodynamic models and has been used in WEC analysis. Hayati et al. [48] studied an oscillating water column converter with the goal of achieving maximum output power in specific wave conditions. Several geometrical parameters were investigated and the results showed an increase in efficiency from 19.75% to 41.5%. The power output of an oscillating water column WEC was also modelled numerically by Lisboa et al. [49] in different wave characteristics using Fluent to determine the power output under those conditions. Particular components of the devices can also be subject to evaluation as did Ozdamar and Pekbey [50] for an oscillating water column converter. In this study, the efficiency of a Wells turbine was determined using Fluent for different cases. The integration of WECs into a breakwater was analysed as well, in the case of rectangular heave buoys, by Zhang et al. [51], using Fluent, as shown in Figure 1.6. As a result it was shown that the performance of the buoys was highly influenced by the submerged depth and also that the absorption efficiency reached 34.2%.

Figure 1.6. Illustration of a floating breakwater composed of heaving buoy WECs [51].

The CFX module of ANSYS is also an alternative for hydrodynamic modelling and for studying the interaction between waves and structures. Bouali et al. [52] analysed an oscillating water column WEC and its geometry optimisation using CFX and another ANSYS tool for geometry modelling and meshing. The parameters used for this evaluation were front wall orientation, immersion depth, and chamber size. The results showed that the front wall immersion depth and chamber size were key parameters in the device's performance, as well as an ideal front wall orientation of 180°. Finnegan and Goggins [53] used ANSYS-CFX to simulate linear waves and the interaction between waves and structures, to assist the design stages of WEC development.

Finally, less implemented than the previous - to the knowledge of the author -, the commercial code Flow 3D also provides tools for hydrodynamic modelling, and has been used in WEC studies. In 2009, Bhinder et al. [54] performed a study on a new concept for a point absorber converter and used three commercial codes to compare their results and optimise the geometry of the device. There was also data from experimental procedures, and the results showed that there was not a great difference between experimental and simulation data for small amplitude waves, noting an increase in this difference with an increase in wave amplitude. Another comparison between simulated and experimental data was done by Mahnamfar et al. [55] regarding an oscillating water column converter, using results from Flow 3D, under regular wave conditions.

The main features of the different software analysed so far is described in Table 1.2 with the purpose of aiding in the choice made for the upcoming studies.

Table 1.2. Reviewed software for hydrodynamic modelling.

SOFTWARE	MODEL	SOLVER	ADVANTAGES	DISADVANTAGES
NEMOH	Linear	Boundary Element Method	Frequency-domain Open-Source Runs in Matlab Simpler configuration	Few test cases in manuals Limit of nodes in mesh generation Struggles with certain levels of geometry complexity
WAMIT	Linear	Boundary Element Method	Frequency-domain Includes irregular frequency removal option Lower computational time	Paid license No embedded mesh generator Limited types of geometries available in subroutines

SOFTWARE	MODEL	SOLVER	ADVANTAGES	DISADVANTAGES
ANSYS AQWA	Linear Non-linear	Boundary Element Method	Frequency-domain Built-in CAD software (Workbench) Supports many geometries	Paid license Struggles with certain nonlinear responses High computational time
WEC-Sim	Linear Non-linear	Boundary Element Method	Time-domain Open-Source Captures nonlinear responses	High computational effort Depends on external frequency-domain code
ANSYS Fluent	Non-linear	Pressure/ Density-based Finite Volume Method	Frequency-domain Time-domain Built-in CAD software (Workbench)	Paid license Requires more input for model definition High computational effort
ANSYS CFX	Linear Non-linear	Finite Volume Method	Frequency-domain Time-domain Built-in CAD software (Workbench)	Paid license Requires more input for model definition Struggles with linear waves
Flow 3D	Linear	Immersed Boundary Method	Frequency-domain May avoid wave reflection	Paid license Requires more input for model definition

1.3.3 *Optimisation process*

To obtain the solutions for the optimisation process, numerical models are a widely used method. There are several conditions to consider before choosing one. If the goal is to study the device's response to small harmonic oscillations, a frequency-domain model can be used for single wave frequencies. However, the superposition of the oscillations of several wave frequencies can be used to calculate the response in irregular seas [12]. The use of time-domain models is generally associated to the inclusion of other non-linear effects. Upon defining a hydrodynamic model and obtaining the needed coefficients, there are several steps going forward in the optimisation process. Initially, there needs to be a clear definition of the objectives. Single-objective optimisation processes involve an objective function that is minimised by a solution that satisfies a number of equality and inequality constraints. On the other hand, a multi-objective optimisation process will seek several solutions for conflicting objective functions, and these solutions will be optimal depending on the importance of each objective function [12].

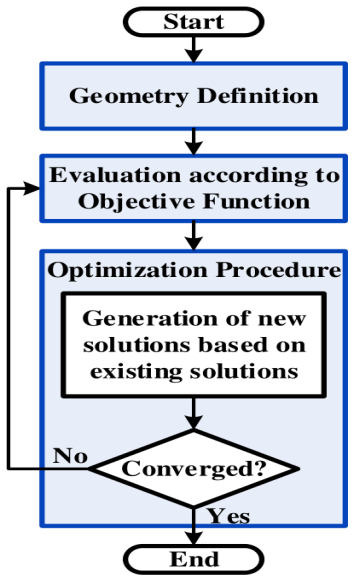

Figure 1.7. Optimisation process for WECs. [12]

The next steps of the process is described in the flow diagram in Figure 1.7. It is possible to identify WEC type and geometry definition as the key elements that will influence the remainder. The decision variables used in this stage will also affect the possible solutions. Besides the chosen variables, the objective function will depend on the models and assumptions made for these variables, for the solution seeking process. Finally, the optimisation procedure relies on the chosen algorithm, since it will affect the computational time, the type of evaluation that can be made, and the convergence to optimal solutions [12].

As mentioned in Section 1.1, there are several types of WECs that can be categorised according to their working principle. There have been studies for a lot of devices, being the point-absorber category the most explored in geometry optimisation. In terms of geometry definition for these devices, the most studied representation is the vertical cylinder, in various shapes [12]. Some of

these shapes are presented in Figure 1.8, where (a) - (h) are vertical cylinders, (i) a sphere, (j) and (k) horizontal cylinders, and the remainder other WEC shapes.

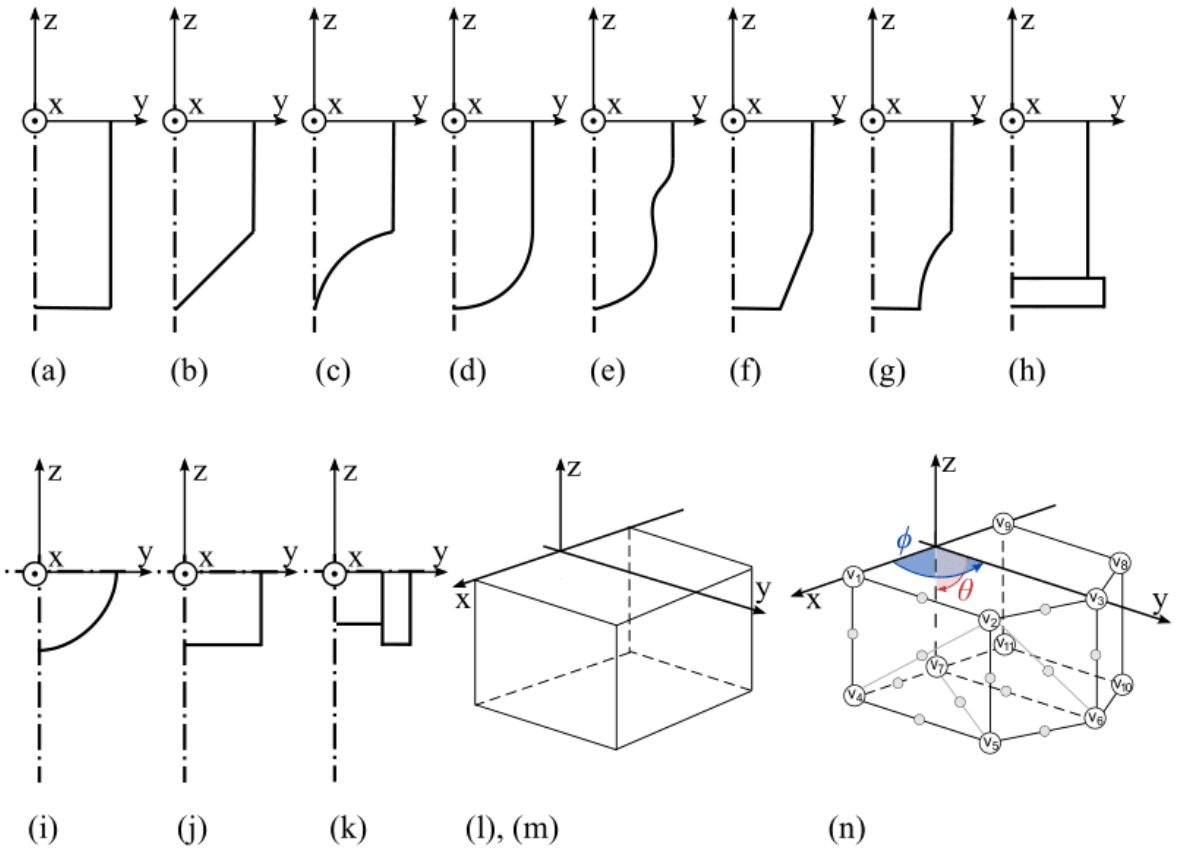

Figure 1.8. Geometry representations from WEC literature [12].

The objective function is the component that is under study, either to be maximised or minimised. This function is dependent on the chosen variables and their values. The purpose of the study will determine both the decision variables and the objective function.

Finding the optimal solution for the objective function may be performed by an optimisation algorithm which will be computed as many times as necessary until the best solution is achieved. There are several types of algorithms that can be used for the purpose of WEC geometry optimisation and these will be reviewed in this section, as well as their application in the context of WEC optimisation.

Primarily, the suitability of a particular algorithm is related to the complexity and type of problem under analysis. Optimisation algorithms are generally included into two major methods: exact and approximate. Optimal solutions are achieved by exact methods,

while approximate methods solve complex problems with good solutions. Gradient-based algorithms are part of the exact methods, as well as direct search methods. Heuristic and meta-heuristic algorithms are included in the approximate methods, and the main difference between both of them is that the first ones generally provide solutions for specific problems, while the latter are developed for more general optimisation problems [12]. Among meta-heuristic methods, some of the most popular algorithms are the genetic algorithms. These are based on evolution theory, which is essentially the survival of the fittest. Initially, a set of random WEC shapes, in this case, is generated from the combination between the variables chosen for the optimisation [56]. The process then evolves to the choice of the best solutions from each iteration of the algorithm which then generate new solutions through combinations until a good enough solution is found for the problem. A schematic of this type of algorithm is found in Figure 1.9.

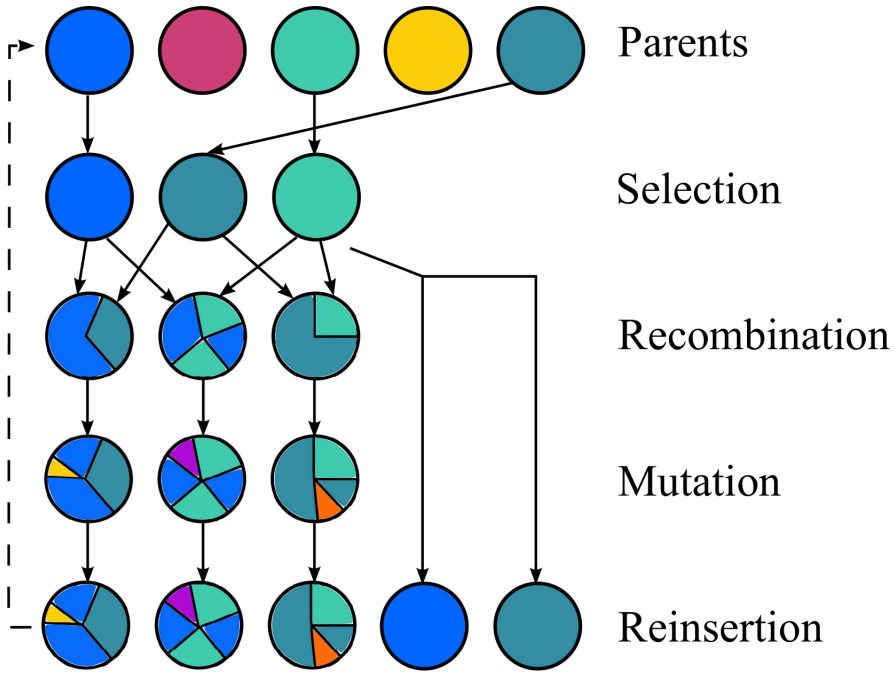

Figure 1.9. Schematics of a genetic algorithm iteration [12].

There have been several studies on WEC optimisation, using different methods. In the case of [57], the analysed device consisted of a sphere-shaped buoy, a fully submerged non-buoyant sphere-shaped supplementary mass, and a PTO hydraulic unit lying on the seabed, as shown in Figure 1.10. The analysis involved applying a control technique to adjust the device's natural period to be resonant with the incident waves. The optimisation was done varying the buoy's diameter and the PTO's external damping. The results allowed

to conclude that the absorbed energy distribution was not significantly different for each configuration when under the same wave conditions, which means that the deployment site is an important parameter to consider when optimising WECs. In 2018, the optimisation of a point-absorber was performed by Shadman et al. [20] considering three main requirements, namely the buoy heave natural frequency, the resonance bandwidth, and the maximum mechanical power, using two geometrical parameters - the buoy diameter and draft. This study was done using the method of design of experiments, defining upper and lower bounds for both geometrical parameters. The evaluation of these variables depended on the resulting buoy heave natural frequency compared with the incident wave's frequency, which was site dependent. As a result, it was found that for one of the analysed locations, there wasn't a combination of diameter and draft values that would reach a desirable natural heave frequency value for the buoy since the wave periods were high, reinforcing the importance of site definition in WEC analysis. Using a genetic algorithm, McCabe [58] optimised a WEC with a reduced number of control points, that would generate the bi-cubic B-spline surfaces and were evaluated through different cost functions. These functions assessed the overall mean power and ratios between this parameter and the length of the shape, as well as its displaced volume. A set of constraints was also applied regarding non-convergences in the BEM code. A population size of 22 and a maximum of 50 generations were set for each run. There was a total of 12 runs, corresponding to the 3 cost functions under the 4 constraints applied (maximum displacement amplitude and PTO power rating). The results showed that considering the size and the mean power delivery in the optimisation process leads to substantially improved performances. A previous study, from 2010 [59], performed the optimisation of a point absorber considering the interaction between the geometry of the device and the control strategy adopted for it. The problem was solved using a deterministic algorithm.

The device SeaWEED, an attenuator, was also optimised regarded its PTO damping and geometrical parameters (draft and length) [40]. The PTO system is hydraulic, and the optimisation was achieved in a total of 250 simulations considering upper and lower bounds for length, draft, and PTO damping. Two steps were taken in the process, starting with the optimisation of the PTO damping value for a defined geometry and then the optimisation of the geometry for determined wave conditions. Another type of device, a floating oscillating water column, was optimised in 2012 [60], focusing on its dimensions as the optimising variables (5 parameters). Regarding the methods applied, two algorithms

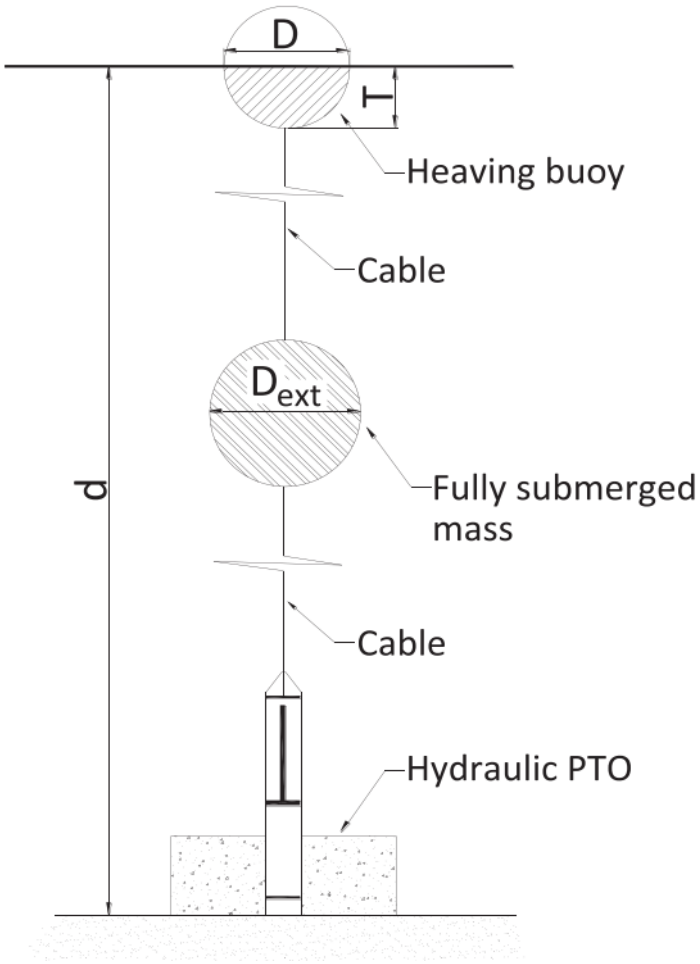

Figure 1.10. Point-absorber layout [57].

were used and compared: a direct search method (COBYLA) and a metaheuristic method (DE). The main goal of the study was to maximise the annual averaged power for the analysed sea states. The results showed that the differences between COBYLA and DE are small, leading to the choice of COBYLA when a faster computation is intended. Bachynski et al. [61] assessed the effects of geometry, mass distribution, and mooring lines on the response of a tethered WEC in irregular waves. It was possible to conclude that the optimisation of different design parameters is essential to tune the device's resonance frequencies to the wave climate at any site.

From the analysis of the different studies mentioned previously, the choice of optimisation method shows great importance not only in terms of efficiency, but also considering the parameters that are under study, and the accuracy sought during the assessment.

1.3.4 *State of the Art*

The development of wave energy to a commercial stage is highly dependent on the viability of the existing devices. Currently, there are several designs for WECs, which is positive in terms of innovation, but leads to a lack of a prevailing concept, which is tested and proved to be reliable at a commercial stage.

Besides this, there is still a high cost associated with both the conception of the devices, where geometry has a great potential to decrease overall costs, and their maintenance, since the ocean provides extreme conditions for these systems. These conditions affect another parameter that influences wave energy growth, which is survivability at sea.

These deficiencies of the sector are being corrected through optimisation studies. These can be performed with the goal of reaching the best design possible to follow to real condition testing, reduce costs in system design and geometry, and build more robust devices for the harsh ocean conditions. Hydrodynamic models are essential tools in this process, since they allow to obtain value for hydrodynamic coefficients that will be used to evaluate the interaction between the waves and the structures.

Although these efforts are being done, there is still a lack of a standardised optimisation process for WECs that could allow for a trustworthy comparison between results from different studies in different wave conditions.

1.4 THESIS CONTRIBUTION

As mentioned in the previous sections, optimisation processes bring several advantages to the development of WECs, from cost reduction to power absorption maximisation. Geometry optimisation acts as a key element in these parameters.

The work developed in this thesis focuses on maximising the energy absorption by the device, possibly working with resonance values with the chosen wave conditions. In this case, a point-absorber converter will be the subject of the study, so the heaving motion of the device will be considered as the main driving force of the energy extraction. Mooring lines are not considered since the main focus is the buoyant structure's interaction, according to its shape.

1.5 STRUCTURE

This document is organised having in consideration the stages of development of the thesis. The chapters include sections and subsections, with the following structure:

- Chapter 1 - *Introduction*
  - This chapter presents the framework and main goals of this thesis, along with a literature review on the topic.
- Chapter 2 - *Numerical Simulation of the Wave Energy Converter*
  - This chapter describes the device considered in this study and the sea states evaluated. The models used for the geometry of the studied WEC and for hydrodynamics are also described.
- Chapter 3 - *Optimisation Process*
  - The optimisation process is shown, presenting the contemplated parameters and algorithm.
- Chapter 4 - *Analysis and Discussion*
  - This chapter presents a discussion of the results from the previous stages.
- Chapter 5 - *Conclusions and Future Work*
  - This chapter presents a set of conclusions from the work developed in this thesis and also some considerations for future work in this subject.

2

NUMERICAL SIMULATION OF THE WAVE ENERGY CONVERTER

The research about the different approaches on WEC optimisation and their description provides tools to define a structured methodology to achieve the intended goal of reaching the best shape for the system. In this chapter, the software choice, theoretical and technical assumptions, as well as the used data, are described.

2.1 WAVE THEORY

Observing the ocean and its strength raises no doubt about the energy its waves contain. To allow this energy to be extracted, the resource must be well understood and studied. Ocean waves used to generate electricity are mostly excited by wind and are generally represented as a sinusoid [62]. There are a few parameters of a wave that can be used to describe it, namely wavelength, λ, corresponding to the distance between two equivalent points in the wave; the wave height, H, corresponding to the distance between the wave crest and the wave trough; and the wave period, T, corresponding to the time the wave takes to travel the distance of one wavelength [62] Figure 2.1.

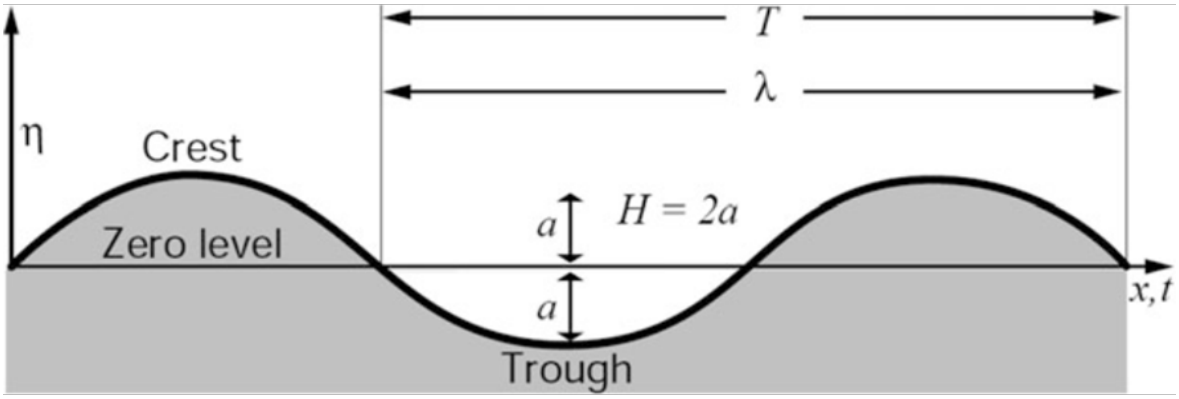

Figure 2.1. Wave characteristics [62].

The modelling of waves and body interaction can be done according to different theories, considering the linearity of the waves. In this study, the chosen software for hydrodynamic modelling is WEC-Sim, using the frequency-domain BEM code NEMOH. Both use linear wave theory as their basis. Linear potential flow theory considers an inviscid

and irrotational flow, which means it has no friction and the fluid has no particle rotation [63]. Every real fluid has viscosity, but under certain circumstances its effect is reduced enough so it can be considered insignificant.

In the case of WEC-Sim, after the frequency-domain linear hydrodynamic coefficients are calculated by an external solver, in this case NEMOH, and then imported in a non-dimensionalised form, they are scaled using the following methods [64]:

$$\overline{|F_{exc}(\omega)|} = \frac{|F_{exc}(\omega)|}{\rho g} \tag{1}$$

$$\overline{A(\omega)} = \frac{A(\omega)}{\rho} \tag{2}$$

$$\overline{B(\omega)} = \frac{B(\omega)}{\rho \omega} \tag{3}$$

$$\overline{C_{hs}} = \frac{C_{hs}}{\rho g} \tag{4}$$

where $\overline{F_{exc}}$ is the normalised wave excitation force, F_{exc} is the wave excitation force, ρ is the water density, g is the gravitational acceleration, $\overline{A}$ is the normalised radiation added mass, $A(\omega)$ is the frequency dependent radiation added mass, $\overline{B}$ is the normalised radiation wave damping, $B(\omega)$ is the frequency dependent radiation wave damping, $\overline{C_{hs}}$ is the normalised linear hydrostatic restoring coefficient, C_{hs} is the linear hydrostatic restoring coefficient, and ω is the wave angular frequency.

Linear wave theory also assumes that a wave is the sum of incidence, radiation, and diffraction components of the wave [64], which aids in the determination of hydrodynamic forces. Calculating the dynamic response of a floating device requires the calculation of the WEC equations of motion, which includes the following, calculated around the centre of gravity of the body:

$$m\ddot{X} = F_{exc}(t) + F_{rad}(t) + F_{pto}(t) + F_{v}(t) + F_{me}(t) + F_{B}(t) + F_{m}(t) \tag{5}$$

where m is the body mass matrix, $\ddot{X}$ is the acceleration vector of the device, $F_{exc}(t)$ is the eave excitation force and torque vector, $F_{rad}(t)$ is the wave radiation force and torque vector,

$F_{pto}(t)$ is the PTO force and torque vector, $F_v(t)$ is the damping force and torque vector, $F_{me}(t)$ is the Morison Element force and torque vector, $F_B(t)$ is the net buoyancy restoring force and torque vector, and $F_m(t)$ is the mooring connection force and torque vector.

The hydrodynamic coefficients provided by NEMOH are used to calculate $F_{exc}(t)$, $F_{rad}(t)$, and $F_B(t)$.

In this case, a linear PTO mechanism is used, and in WEC-Sim it is represented as a linear spring-damper system.

According to the documentation available, the reaction force of this system is given by [64]:

$$F_{PTO} = -K_{PTO}X_{rel} - C_{PTO}\dot{X}_{rel} \tag{6}$$

and the instantaneous power absorbed by the system is given by:

$$P_{PTO} = -F_{PTO}\dot{X}_{rel} = \left(K_{PTO}X_{rel}\dot{X}_{rel} + C_{PTO}\dot{X}_{rel}{}^2\right) \tag{7}$$

where F_{PTO} is the PTO system reaction force, K_{PTO} is the stiffness of the PTO system, X_{rel} is the relative motion between the two bodies, C_{PTO} is the damping of the PTO system, $\dot{X}_{rel}$ is the relative velocity of the two bodies, and P_{PTO} is the PTO power absorbed by the PTO system.

2.1.1 *Spectral analysis*

A determined sea state can be represented by its wave spectrum. This spectrum is used to describe the energy distribution along several frequencies. There are different ways to calculate this distribution, and in this study the Pierson-Moskowitz (PM) method was used.

The PM spectrum definition contemplated was provided by WEC-Sim, and is based on two parameters: H_s and T_p. In this formulation, it is considered that the spectral density of the surface elevation is given, according to the IEC standards [65], by:

$$S_{PM}(f) = \frac{H_s{}^2}{4}(1.057f_p)^4 f^{-5} exp\left[-\frac{5}{4}\left(\frac{f_p}{f}\right)^4\right] \tag{8}$$

and assuming the following wave spectrum coefficients:

$$A_{ws} = \frac{{H_s}^2}{4}\left(1.057 f_p\right)^4 \approx \frac{5}{16}{H_s}^2 {f_p}^4 \approx \frac{B_{ws}}{4}{H_s}^2 \tag{9}$$

$$B_{ws} = \left(1.057 f_p\right)^4 \approx \frac{5}{4}{f_p}^4 \tag{10}$$

where $S_{PM}(f)$ is the PM spectrum, f_p is the wave peak frequency, f is the wave frequency, and A_{ws} and B_{ws} are the wave spectrum coefficients.

2.1.2 *Hydrodynamic forces on offshore bodies*

The effect of ocean waves on floating and moored bodies is expressed through the forces acting on them. These forces can be divided in two categories: hydrodynamic/hydrostatic (external) loads and reaction forces [63]. More specifically, the external loads acting on these systems are:

- Hydrostatic force - the oscillation of the device leads to a difference in the distribution of hydrostatic pressure, which is expressed by this force.
- Excitation forces - caused by the impact of incident waves on a stationary body.
- Radiation forces - the oscillatory motion of the device displaces the fluid around it, causing a variation in the pressure field, in an interval of incident waves. The radiation forces are then experienced by the device due to this phenomenon.

  The reaction forces, which may vary due to the type of WEC, include [63]:

- PTO forces - caused by the PTO system, responsible for the conversion of the mechanical energy from the movement of the device.
- Mooring/foundation forces - these are due to the equipment that keeps the device steady.

Besides these, there is also the added mass coefficient, which regards an increase in inertia caused by the displacement of water in the surroundings of the body when it moves, the damping coefficient, corresponding to the energy dissipated to the water caused by the oscillations propagating away from the float, and restoring coefficients that refer to the forces that put the float back to its equilibrium position [63].

2.2 STRUCTURAL MODEL

The WEC was modelled in WEC-Sim [66], using the Simulink library associated to it. Its representation is presented in Figure 2.2. The model was based on the RM3 application made available by the developers. The RM3 is also a point-absorber, although represented with two bodies. In this case, the studied WEC was considered solely with a floating buoy and a PTO system. Mooring configurations were not considered since they exceed the study's focus. The buoy's top radius was set to 5 m, and the draft to 10 m.

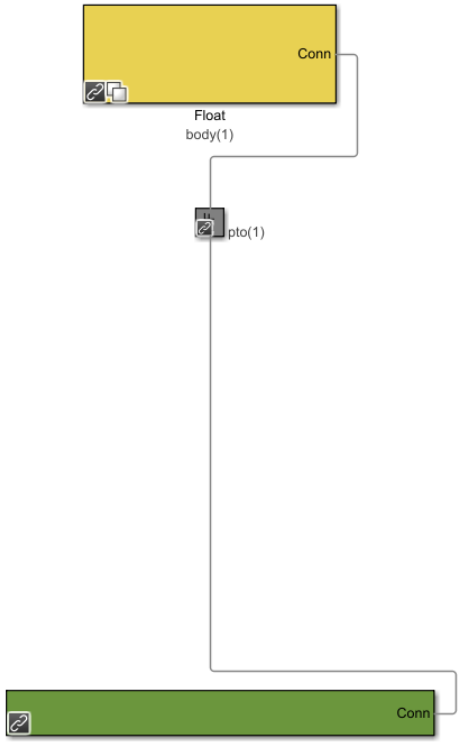

Figure 2.2. Simulink model for the case study device.

Since the main goal is to optimise the shape of the buoy, it is also important to consider the mesh fed to NEMOH, which will determine the following analysis through WEC-Sim. The initial shape designed was similar to a ship's hull, as represented in Figure 2.3. Considering the results from [28], conical shapes perform better than cylinder shapes, which influenced the choice for this first shape. For NEMOH, it is only important to represent the submersed part of the device, as is noticeable by the z-axis in Figure 2.3.

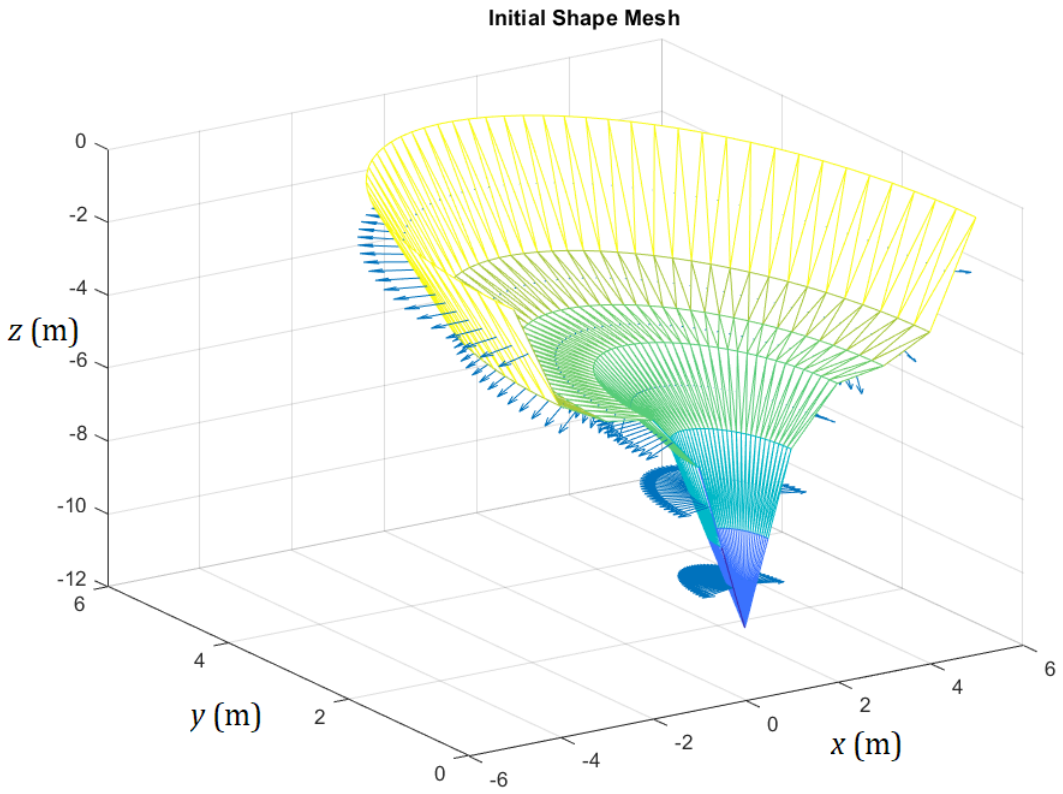

Figure 2.3. NEMOH mesh for the initial simulation.

2.3 SEA CHARACTERISTICS

The data used in WEC-Sim regarding wave conditions was taken from the Global Ocean Waves Analysis and Forecast data set from the database Copernicus [67]. This data is the result of a spectral analysis of wave parameters, with a temporal resolution of 3 hours. The set of data downloaded corresponded to the year of 2020. The chosen site was offshore of Viana do Castelo, Portugal, as represented in Figure 2.4. This location was chosen since it is going to be the deployment site for a commercial stage point-absorber. The data was analysed, and different wave conditions were determined.

The extracted data involved the following parameters:

- Significant wave height, H_s - mean of the highest one third of waves in a particular series [68].
- Peak period, T_p - period corresponding to the most energetic waves in a wave spectrum [69].
- Mean wave direction, θ - direction from which the waves are coming from.

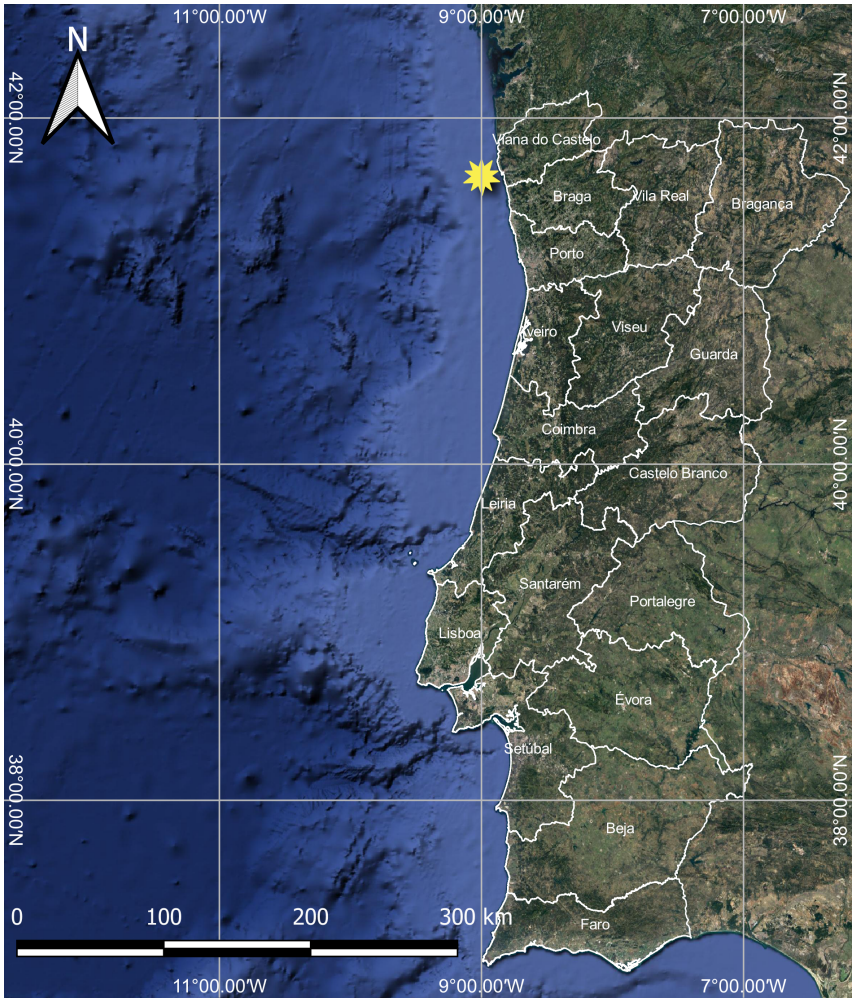

Figure 2.4. Map with chosen site for the wave data.

The time series of the extracted parameters are shown in Figure 2.5-Figure 2.7, with the corresponding root mean square values.

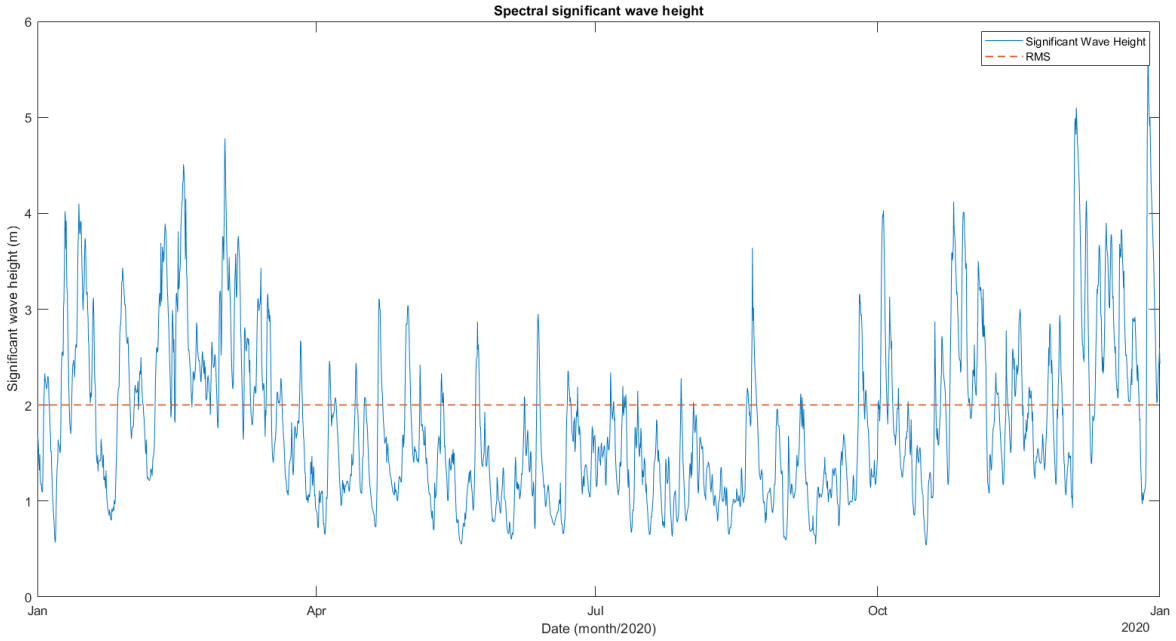

Figure 2.5. Wave significant height for the chosen site.

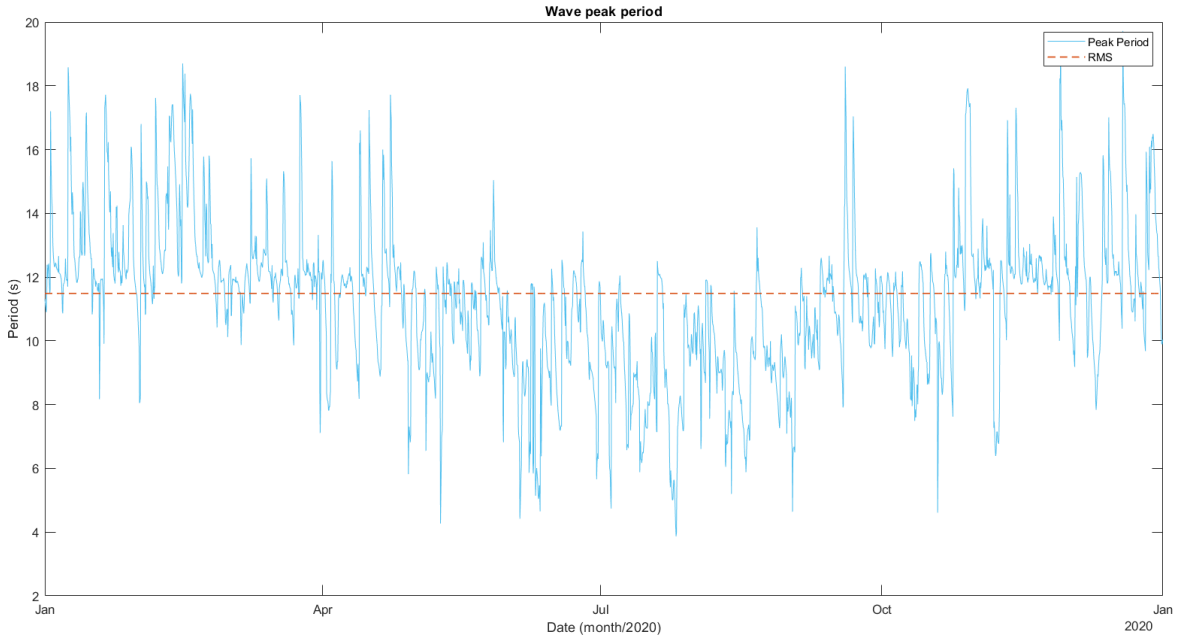

Figure 2.6. Wave peak period for the chosen site.

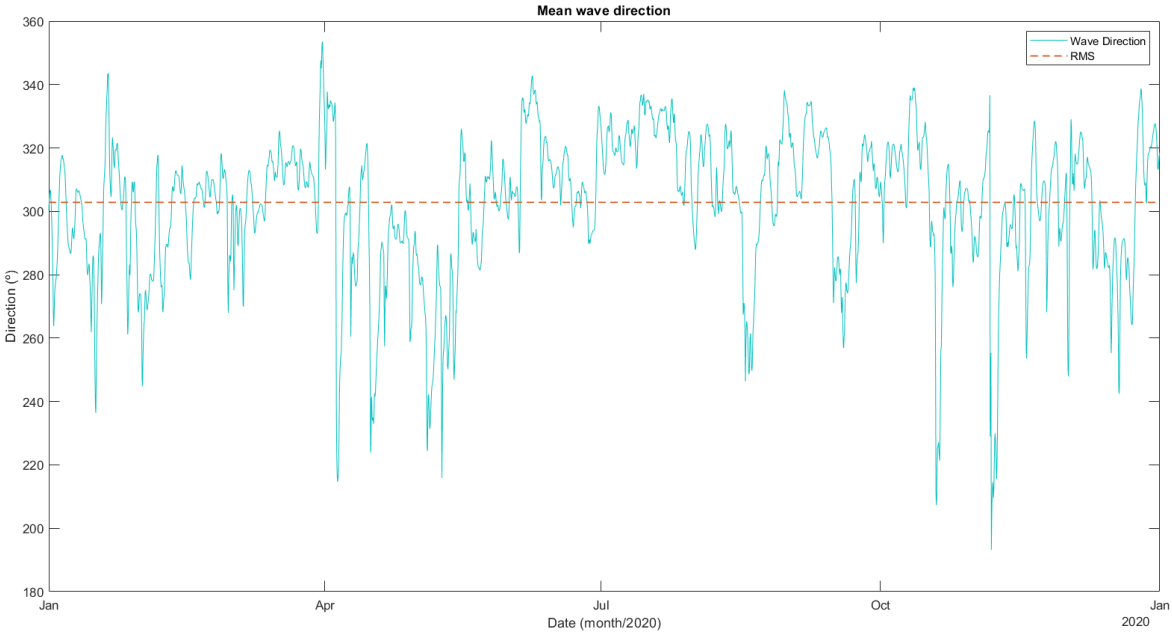

Figure 2.7. Mean wave direction for the chosen site.

The PM spectrum associated to the values used for extreme wave conditions - H_s = 4.78 m and T_p = 10.82 s - is represented in Figure 2.8.

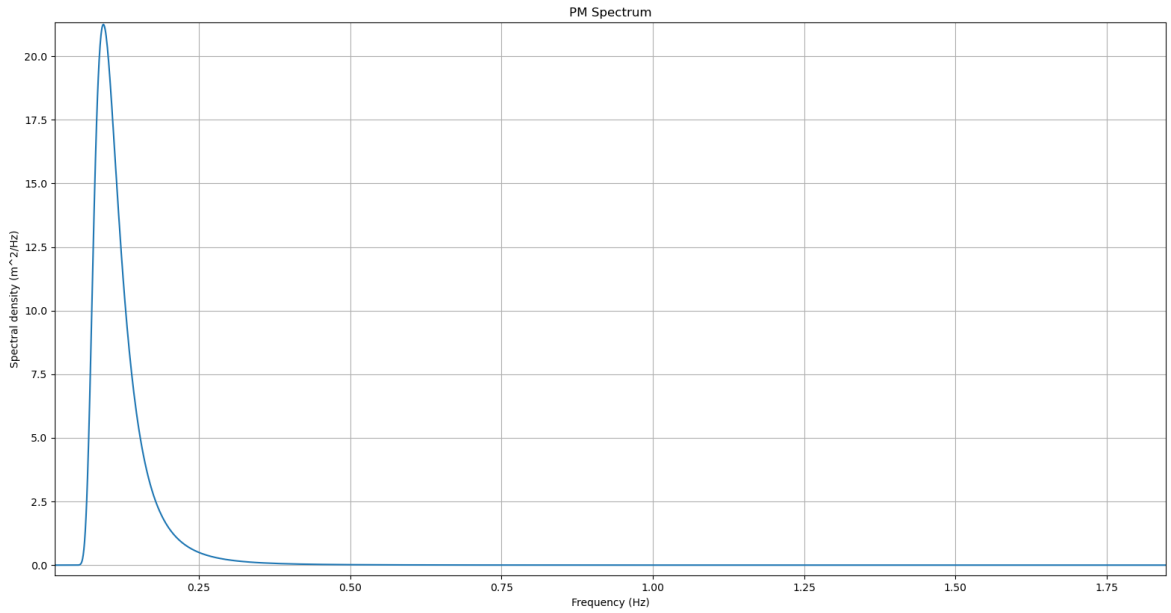

Figure 2.8. Pierson-Moskowitz spectrum for the considered extreme wave conditions.

2.4 HYDRODYNAMICS MODEL

Among the different frequency-domain BEM codes available, NEMOH [31] stood out as a reliable open-source code for obtaining the required hydrodynamic coefficients. The other options for input to WEC-Sim required a paid license. There is also the advantage of a high user scope due to its availability, which helps solving possible issues during its use. Its programs and their functionality are described in Figure 2.9. The programs are run using the MATLAB wrapper provided by the developers.

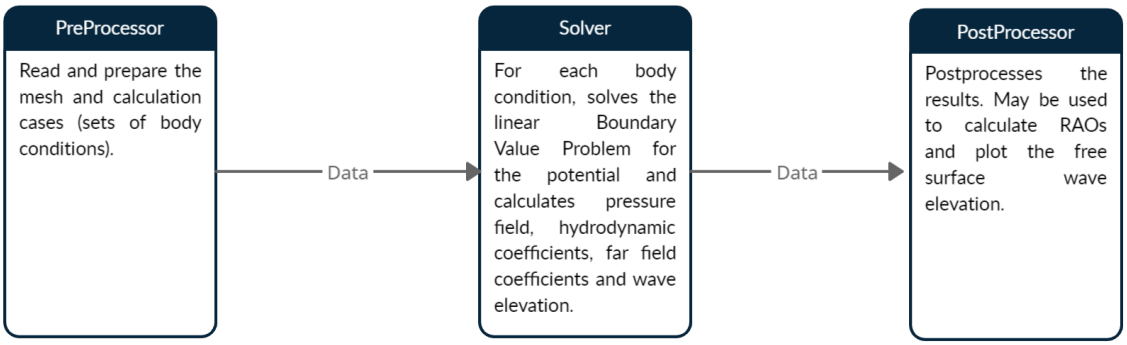

Figure 2.9. NEMOH programs, adapted from [31].

The input values for NEMOH include:

- Buoy mesh - the mesh of the submerged part of the buoy is defined through a function, either axisymmetric or not. In this case, the axisymmetric option was used, requiring the following inputs:
  - Array of radial coordinates (r)
  - Array of vertical coordinates (z)
  - Number of points for discretisation (n)

  Besides these initial inputs, the function then requires the user to manually introduce the remainder values, after it is already running. This is a particular problem if the process is to be automated. Therefore, a few modifications to the source code were made, and the following parameters were defined as initial inputs as well:
  - Number of points for angular discretisation (*ntheta*)
  - Directory name for storing the results (*nomrep*)

  - Vertical position of the centre of gravity (zG)
  - Target for number of panels (*nfobj*)

  The function then produces the following outputs:

  - Mass of the buoy
  - Inertia matrix, which is estimated assuming the mass is distributed on the wetted surface
  - Hydrostatic stiffness matrix
  - Coordinates of the buoyancy centre

- Wave characteristics:
  - Vector of wave angular frequencies (ω) [rad/s]
  - Wave direction [degrees]
  - Water depth [m]

The outputs of NEMOH are then analysed through a BEM input/output function, part of the WEC-Sim software package, to transform them into readble inputs for WEC-Sim. This function is called BEMIO (Boundary-Element Method Input/Output) and builds a .h5 file with the results.

WEC-Sim formulates the study problem in the time domain, and is a useful open-source tool for the case study analysis. It is developed in MATLAB and Simulink, with the structural model developed with the WEC-Sim Simulink library blocks, as represented in Figure 2.2. WEC-Sim is run through the modification of the template WEC-Sim input file.

In terms of input, this file requires the following:

- Simulation Data
  - Simulink model file (.slx)
  - Simulation start time [s]
  - Wave ramp time [s]
  - Simulation end time [s]
  - Chosen solver
  - Simulation time-step [s]

- Wave information
  - Wave class (regular/irregular, among other options)

    Since the only two classes used in this study are 'Regular' and 'Irregular using PM Spectrum', only these two will be described.

    Regular waves

    * Wave class - in this case set to 'regular'
    * Wave height [m]
    * Wave period [s]

    Irregular waves using PM spectrum

    * Wave class - in this case set to 'irregular'
    * Significant wave height [m]
    * Peak period [s]
    * Wave direction [degrees]
    * Wave spectrum type - in this case set to 'PM'

- Body data
  - Create the body variable and number, and set the location of the .h5 file
  - Geometry file (.stl) - only important when using nonlinear hydro options, or for animation purposes
  - Body mass - option 'equilibrium' sets mass to the Displaced Water Weight
  - Body moment of inertia [kg m^2]

- PTO and constraint parameters
  - Inclusion of constraints such as joints
  - *PTO*

    * Initialising the PTO class
    * PTO stiffness [N/m]
    * PTO damping [N/(m/s)]
    * PTO location [m]

The output from WEC-Sim is a MATLAB structure with the following parameters:

- Wave output
  - Time [s]
  - Elevation [m]
- Body output
  - Time [s]
  - Body position in the six Degrees of Freedom (DOF) [m]
  - Body velocity in the six DOF [m/s]
  - Body acceleration in the six DOF [m/s^2]
  - Total force on the body in the six DOF [N]
  - Excitation force on the body in the six DOF [N]
  - Radiation damping force on the body in the six DOF [N]
  - Added mass force on the body in the six DOF [N]
  - Restoring force on the body in the six DOF [N]
  - Morison and viscous forces on the body in the six DOF [N]
  - Linear damping force on the body in the six DOF [N]
- PTO output
  - Time [s]
  - PTO system position in the six DOF [m]
  - PTO system velocity in the six DOF [m/s]
  - PTO system acceleration in the six DOF [m/s^2]
  - Total force on the PTO system in the six DOF [N]
  - Actuation force on the PTO system in the six DOF [N]
  - Constraint force on the PTO system in the six DOF [N]
  - Internal mechanics force in the six DOF [N]
  - Internal mechanics power in the six DOF [W]

The six DOF referred in the output structure of WEC-Sim are described in Figure 2.10, and include heave, yaw, surge, roll, sway, and pitch.

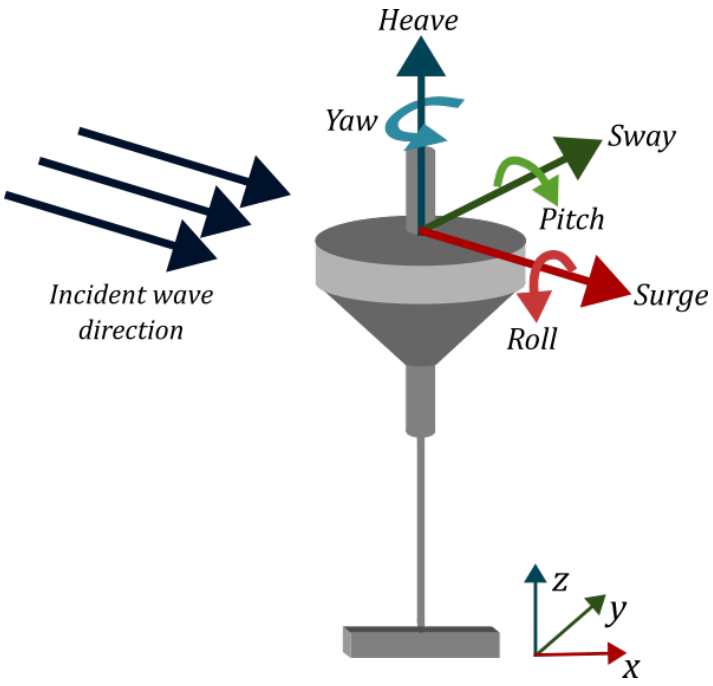

Figure 2.10. Schematics of the six degrees of freedom of a WEC, adapted from [64].

2.5 SIMULATOR ARCHITECTURE

Upon defining NEMOH and WEC-Sim as the software packages, a study workflow was designed (Figure 2.11). One of the main goals when choosing the used software was to consider as much open-source code as possible not only because it would be cheaper, but because it would be more easily reproducible and evolve for different applications.

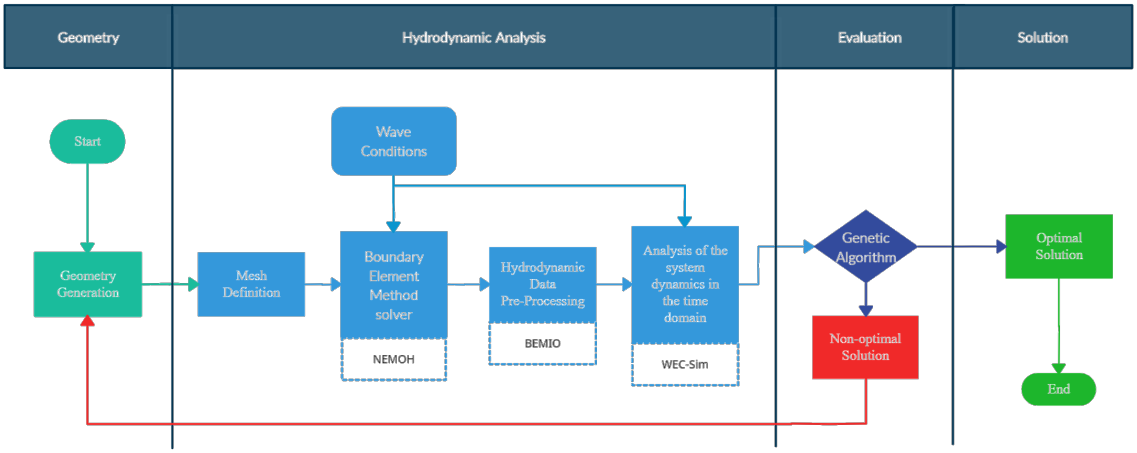

Figure 2.11. Study workflow.

This was achieved as much as possible using the referred packages. However, since their code and simulator depend on MATLAB, which is a paid software, there are a few limitations to possible contributors without access to it.

2.6 SYNTHESIS

The chosen software packages are both based on linear potential flow theory, and for the evaluated cases it is a good approximation since nonlinear effects are not considered in this study. NEMOH is the frequency-domain BEM code used to calculate the problem's hydrodynamic coefficients that WEC-Sim needs for its time-domain formulation and to calculate the outputs. The wave data was taken from a European database and allows to assess the wave conditions in the chosen site. The next steps involve describing the optimisation algorithm chosen for this process.

3

OPTIMISATION PROCESS

Chapter 2 consisted of the description of the theory supporting the hydrodynamic and structural models used, and the software packages chosen for this study. In this chapter, the goal is to present the optimisation methods considered and the motive for choosing the used methodology.

3.1 OPTIMISATION ALGORITHM

As briefly mentioned in Chapter 1, there are several types of optimisation algorithms. Their suitability is dependent on the type of study being developed, its complexity and scope, and the main goals. Considering that in this study a wider scope is intended, a genetic algorithm was chosen to perform the optimisation and find a global minimum instead of local minima.

In this case, the Global Optimisation Toolbox provided in MATLAB was used, particularly the genetic algorithm included in it [70]. The genetic algorithm can be used to solve constrained and unconstrained optimisation problems. As mentioned in Chapter 1, this type of algorithm copies the natural selection process from biological evolution. It keeps modifying the individuals in each population and selecting them randomly to produce the next generations. Each individual is given a fitness value and then the population evolves through generations reaching an optimal individual - the final solution.

There are different methods the genetic algorithm uses to create each population and generate each individual, considering the previous ones [70]:

1. Crossover - two parent individuals are combined to generate the children of the next generation.
2. Mutation - the parents are randomly changed to generate the children.
3. Selection - the parents contribute to the next population.

The genetic algorithm requires the definition of the fitness function, which is the one subjected to optimisation. This function is then applied to each individual and a fitness value is attributed to it. Since the algorithm searches for a minimum of the fitness function, the best solution is found in an individual with the lowest fitness value. An array of individuals forms a population, which is evaluated in each iteration to generate the next population, forming a new generation.

The individuals of the initial population are created using random values, if there is no assigned initial population. Considering the fitness values of each evaluated individual, the next populations are generated. The ones with lower values are considered "elite" and pass to the next population. New individuals are also created from previous ones regarding their expectation, and a new generation is born. This process can be observed in Figure 3.1.

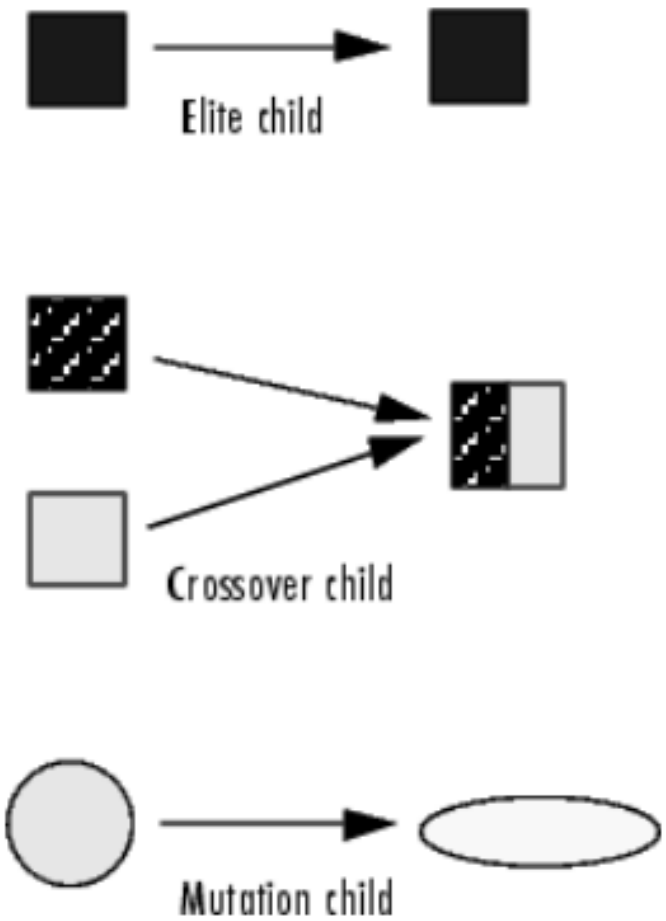

Figure 3.1. Generation of new individuals [70].

3.2 EVALUATED PARAMETERS & FITNESS FUNCTION

For the optimisation process to require less computational effort and time, a limited number of variables are considered as the parameters to be evaluated. Since the goal is to optimise the geometry of the device, the key is to chose the initial values given to NEMOH to define the mesh of the body.

Considering this condition, the array of radial coordinates is chosen as the variable. Six points were used for the generation of the mesh, with radial and vertical coordinates. The radial coordinates were fed to the fitness function to generate the vertical ones according to a function, with two fixed points. Therefore, only 4 points were changed in each iteration. Figure 3.2 shows the fixed points in the red circles, and the changing ones in the green circles.

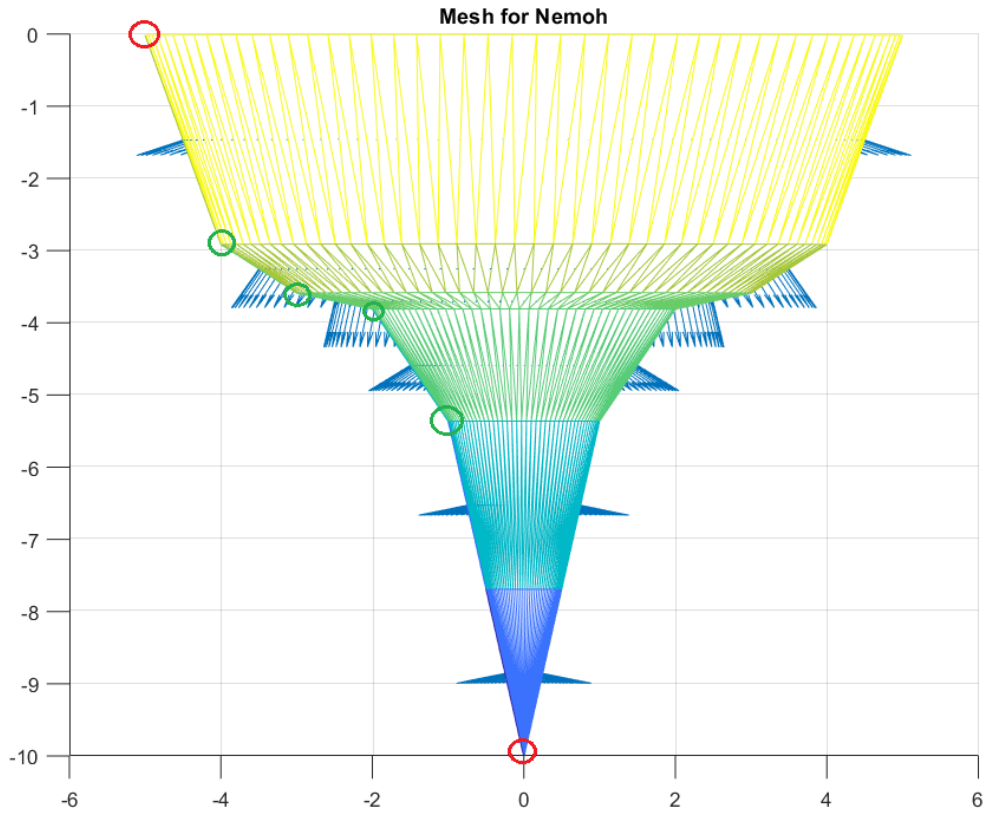

Figure 3.2. Example of a mesh generated with two fixed points.

The fitness function was built weighing the main goals of the study. One of them is to reduce the surge and pitch forces (acting on a heaving device), and increase the heave

forces. Also, it is important to consider the values of the power absorbed by the PTO system. Therefore, the function follows the following distribution:

$$f = 0.15F_{TS} + 0.15F_{TP} - 0.4F_{TH} - 0.3P_{PTO} \tag{11}$$

where F_{TS} is the total surge force, F_{TP} is the total pitch force, F_{TH} is the total heave force, and P_{PTO} is the PTO absorbed power. This distribution was chosen considering the importance of each goal.

3.3 SYNTHESIS

The genetic algorithm was considered an attractive method to develop the optimisation since it allows for a wider scope of solutions evaluated, and even solutions that wouldn't be contemplated when searching for local minima. The generation of different populations from previous ones, according to their fitness, also turns the process more efficient since a main path may be chosen but other individuals are continuously being evaluated, broadening the whole process.

4

ANALYSIS AND DISCUSSION

After determining the main steps for the optimisation problem, the simulations were defined. In this chapter, their results are presented and discussed. The optimisation algorithm was run with the goal of achieving the best shape under the fitness function described in Chapter 3. However, there were several aspects to consider when defining the main parameters for the optimisation. Therefore, several simulations were made to provide some validation to the results in terms of mesh refinement, wave conditions, and initial shape. The main results of these simulations are described in the following sections.

4.1 VALIDATION

The mesh definition in NEMOH requires settings such as number of panels, and number of points for discretisation of the shape. Initially, to define these parameters properly, the impact of the mesh precision on the results was investigated. Three simulations were made, defined in Table 4.1. The wave conditions were considered regular, with a 2.5 m wave height, and 8 s period. The simulation time in this case, as well as the next ones, was set to 400 s. The meshes generated are represented in Figure 4.1.

Table 4.1. Characteristics of the validation simulations.

	SIMULATION 1	SIMULATION 2	SIMULATION 3
NUMBER OF POINTS	6	11	6
TARGET NUMBER OF PANELS	500	300	300

The results showed that there was no significant difference in the definition of the mesh, either using a higher value for the number of panels or for the number of points for discretisation. Figure 4.2 - Figure 4.4 show the difference between the three simulations

regarding body position, velocity, and heave total force respectively. Table 4.2 summarises these results and the effect of using a coarser mesh.

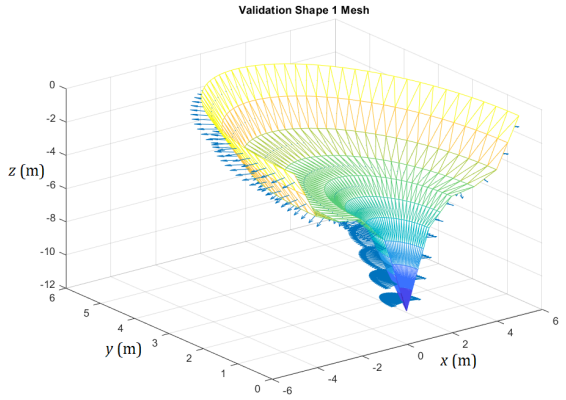

(a) First validation simulation shape.

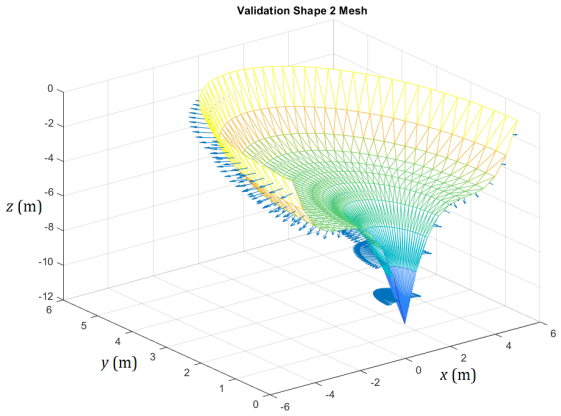

(b) Second validation simulation shape.

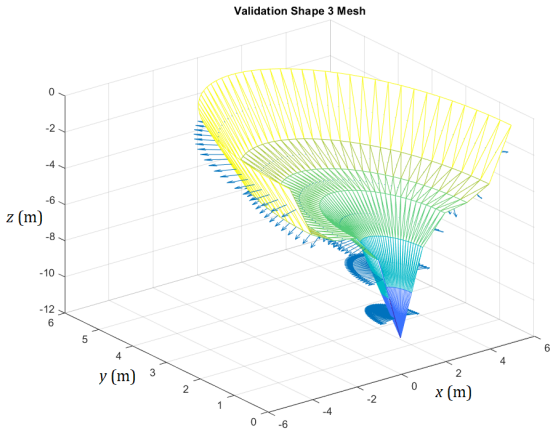

(c) Third validation simulation shape.

Figure 4.1. Validation simulation shape meshes.

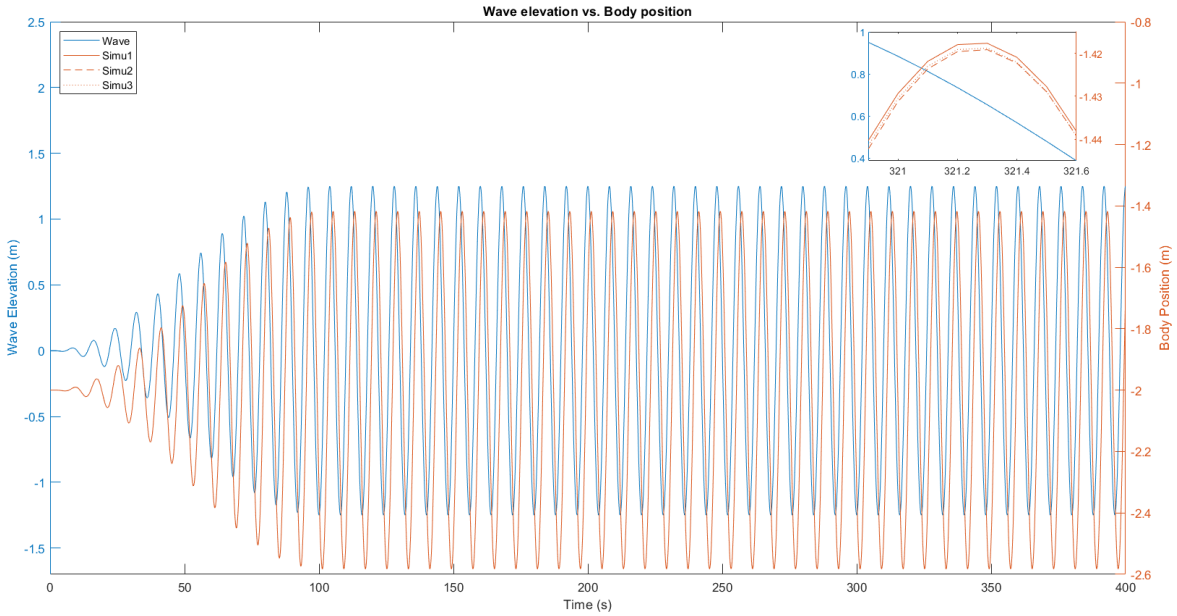

Figure 4.2. Body position for the three validation simulations, zoomed for line distinction.

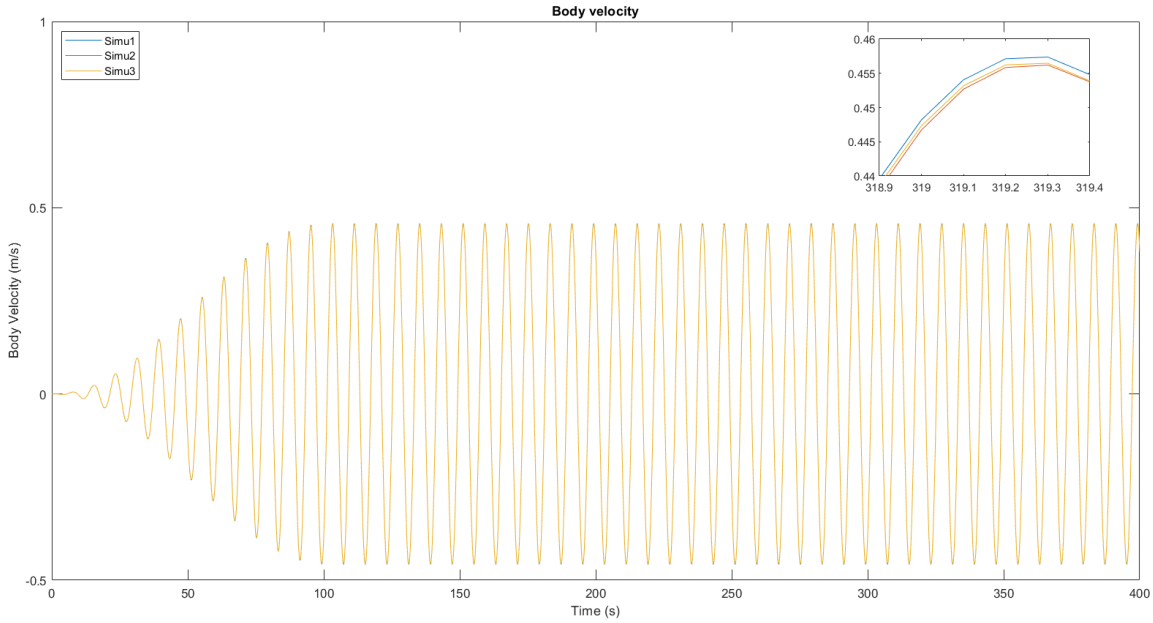

Figure 4.3. Body velocity for the three validation simulations, zoomed for line distinction.

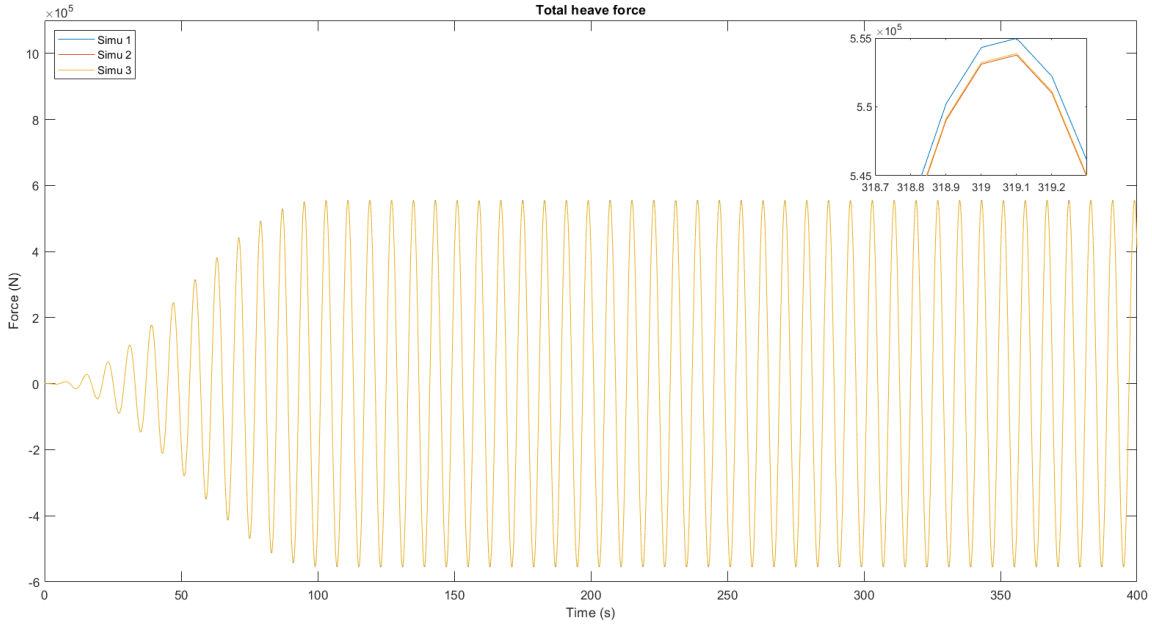

Figure 4.4. Body heave total force for the three validation simulations, zoomed for line distinction.

Table 4.2. Results from the validation process.

	SURGE FORCES (%)	HEAVE FORCES (%)	PITCH FORCES (%)	ENERGY (%)
SIMULATIONS 1-2	1.91	0.00	0.88	0.72
SIMULATIONS 2-3	1.25	0.00	3.49	0.72
SIMULATIONS 1-3	0.64	0.00	2.64	0.00

It is possible to conclude that using a coarser mesh produces good results when compared to a finer one, either through the increase of target number of panels or number of points. Therefore, the meshes in further simulations will be coarser as to save computational time and effort.

4.2 OPTIMISATION RESULTS

After the mesh validation, the optimisation simulations were run. Three particular conditions were tested: optimisation under irregular waves (extreme conditions), optimisation with a cylinder as initial shape, and result testing under average wave conditions. The results are presented in this section.

4.2.1 *Irregular Waves*

The genetic algorithm was run using the WEC-Sim model under irregular waves. Wave conditions were chosen using the data from the climate model described in Chapter 2, and the values were determined exploring this data and searching for an extreme sea state. Choosing this type of sea state helps determine maximum values of energy extraction while also showing how the device performs in a harsher environment. The settings for the algorithm were a maximum of 100 generations, and a population size of 10. The maximum of stall generations was also defined and given a value of 5. The initial shape's mesh is presented in Figure 2.3. The solution which gave the best result of the cost function was achieved at the 957^{th} iteration, with a shape as described in Figure 4.5, and results from this improvement can be seen in Figure 4.6-Figure 4.10.

The main comparison between the two shapes was made considering the root mean square of each of the parameters. There was an increase in the total force in the three degrees of freedom analysed (surge, heave, and pitch), as well as in PTO power and energy. The values are shown in Table 4.3. Although one of the goals was be to decrease the forces in surge and pitch, given that the increase in heave was higher and that it is around ten times the magnitude of the former, the results are considered positive. It is also important to note that there are two x-axes in the body position graph, the left one corresponding to the wave elevation, and the right one to the body's position. While the wave elevation ranges from -5 to 5 m, the body's position, with the graph centred at its centre of gravity, only ranges from -4.5 to 0.5 m, which is about half of the range of the wave elevation.

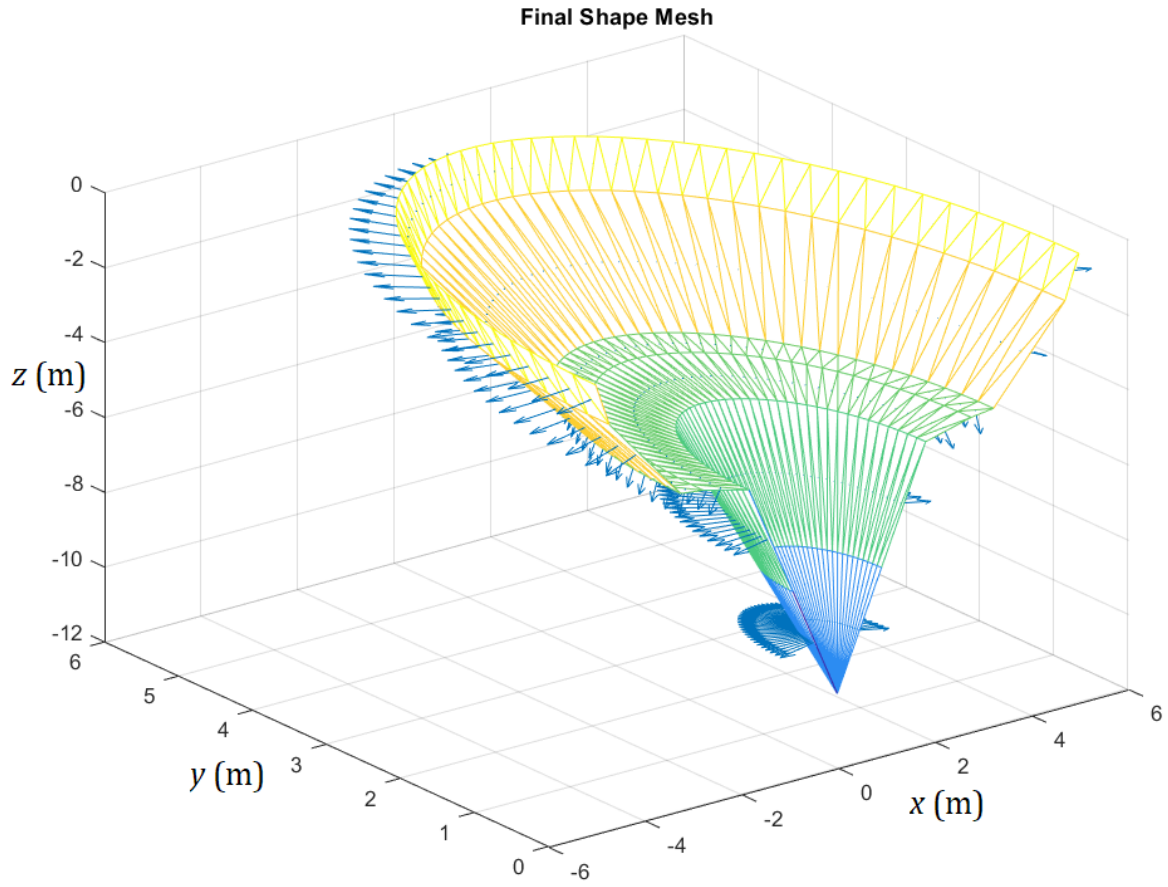

Figure 4.5. Shape obtained after 957 iterations of the genetic algorithm.

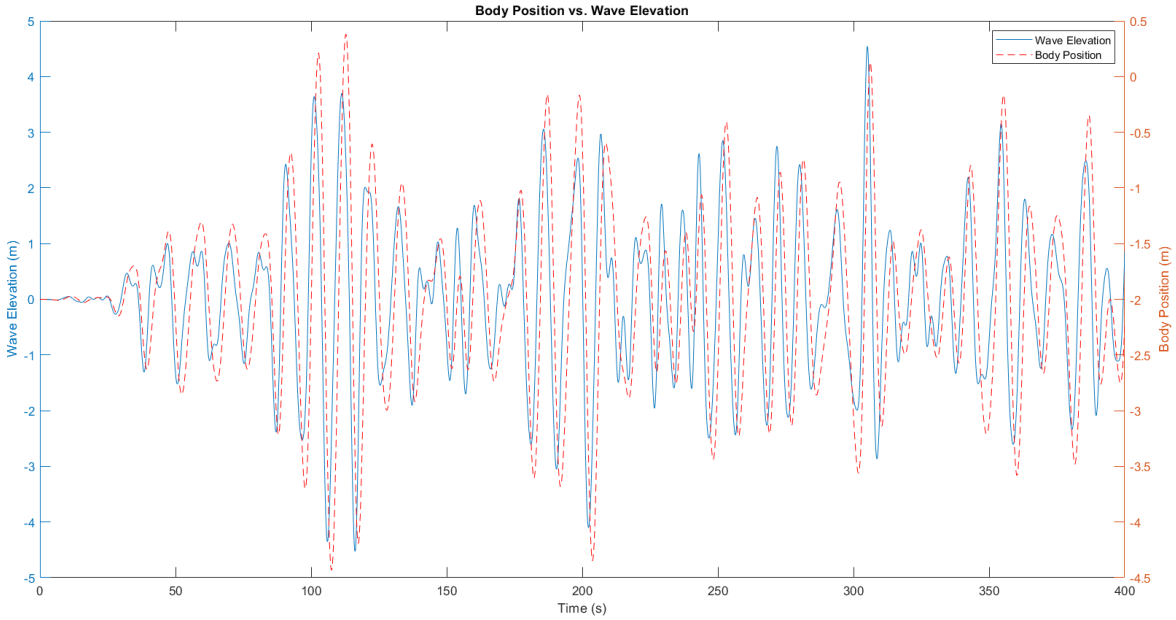

Figure 4.6. Body position of the resulting shape.

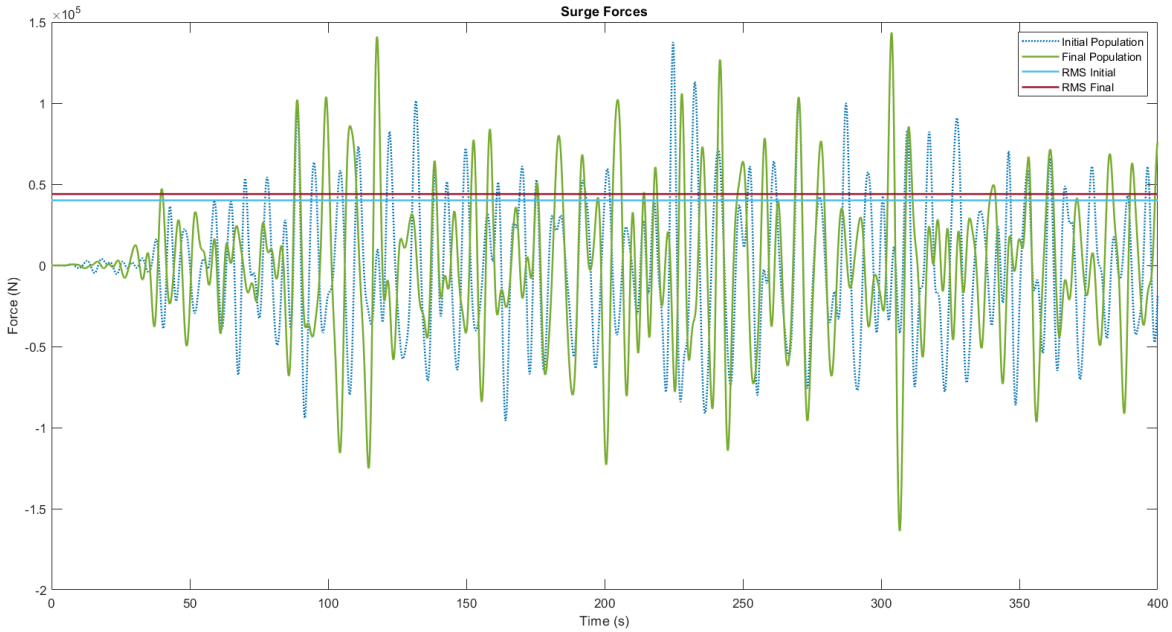

Figure 4.7. Surge total force result for the final shape.

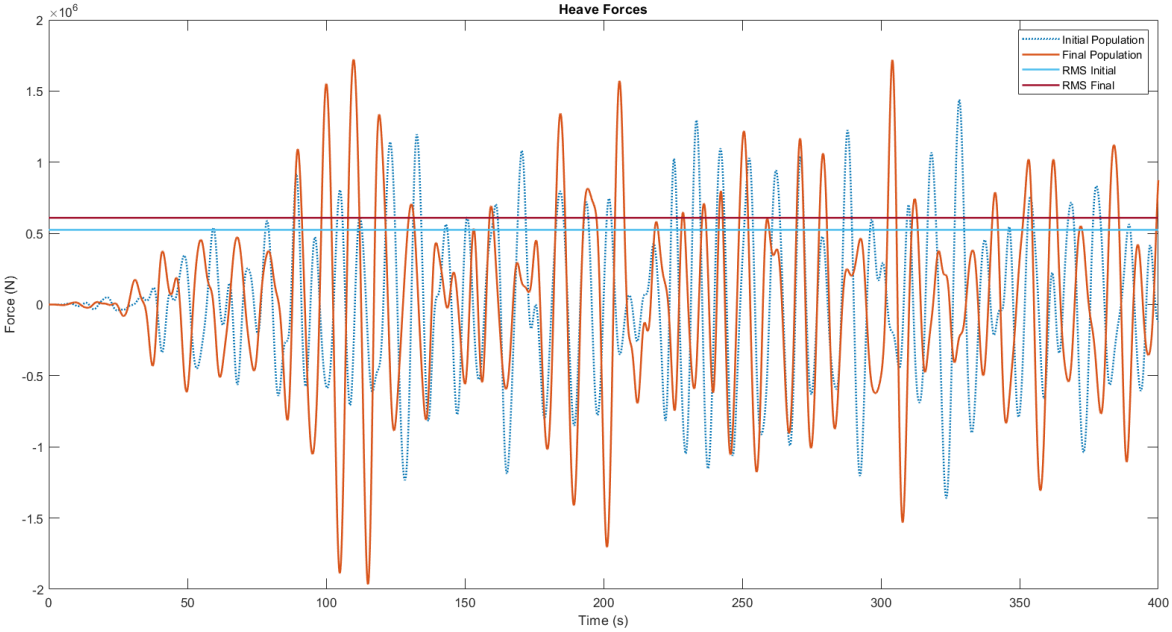

Figure 4.8. Heave total force result for the final shape.

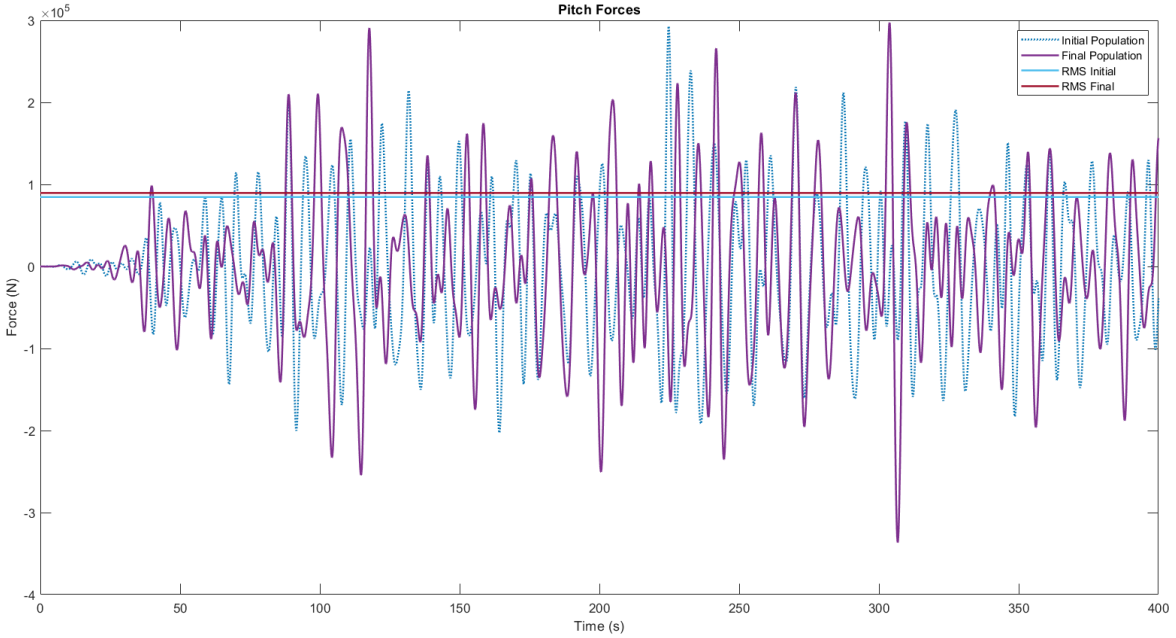

Figure 4.9. Pitch total force result for the final shape.

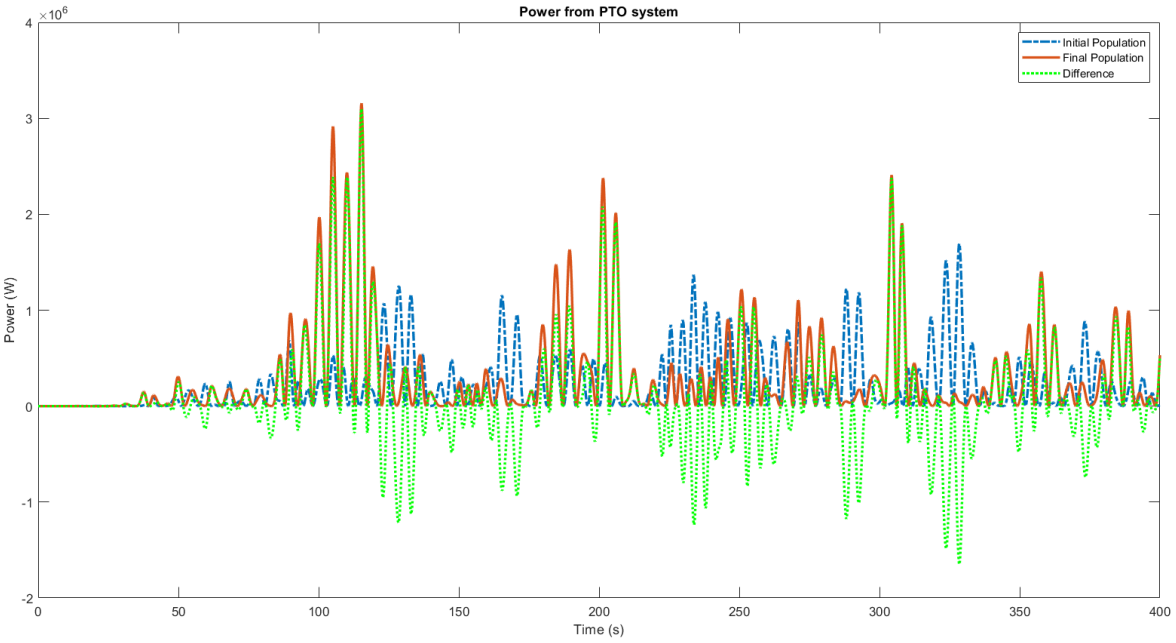

Figure 4.10. PTO absorbed power for the final shape.

Table 4.3. Results from the optimisation process under irregular waves.

	SURGE FORCES (N)	HEAVE FORCES (N)	PITCH FORCES (N)	PTO POWER (W)	ENERGY (kWh)
INITIAL SHAPE	4.00×10^4	5.25×10^5	8.46×10^4	3.71×10^5	41.26
FINAL SHAPE	4.40×10^4	6.09×10^5	8.95×10^4	5.64×10^5	62.72
VARIATION	10.00 %	16.00 %	5.79 %	52.02 %	52.02 %

Table 4.3 also shows an increase of 52.02 % in energy absorption, which is weighed as a more important factor than the impacting forces. After analysing these results, the impact of the first shape fed to the algorithm was also investigated, to see if the final shape was similar, or even the same as the one in this simulation. The results are described in the next section.

4.2.2 *Cylinder Case Study*

In order to know whether the first shape chosen for the algorithm run leads to a very different result, an initial cylinder shape was introduced in NEMOH, presented in Figure 4.11. The wave conditions remained the same as in the previous section, as well as the cost function.

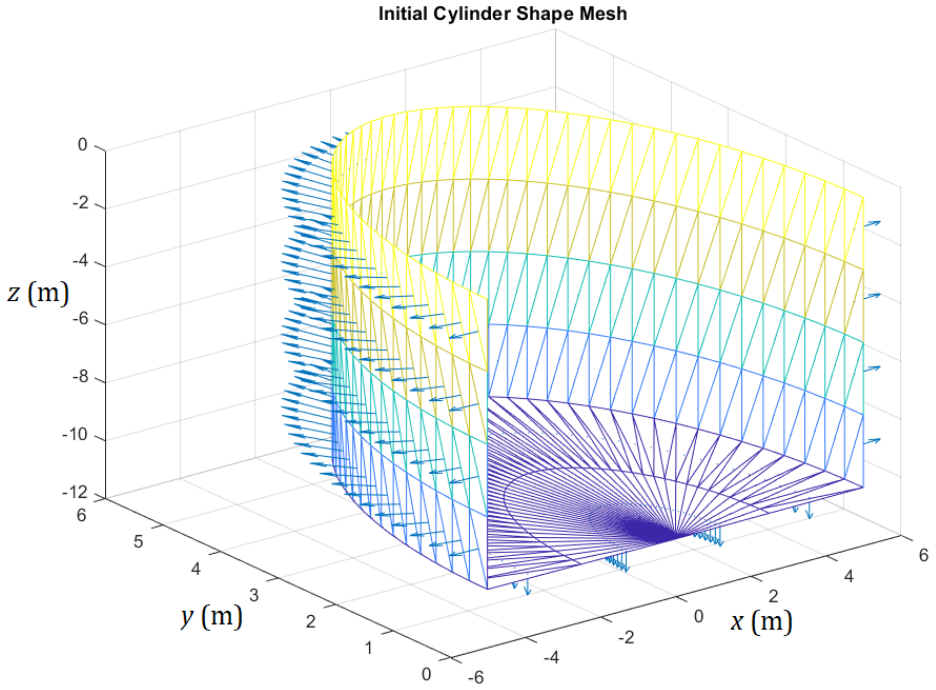

Figure 4.11. Initial shape mesh for the cylinder case study.

The settings for this algorithm run were also the same as the previous, with a maximum of 100 generations and 5 stall generations, and a population size of 10. The best results were obtained after the 665^{th} iteration and are described in Figure 4.13-Figure 4.17 and Table 4.4.

The final shape, as presented in Figure 4.12, is similar to the one resulting from the previous run, in Figure 4.5. The results were slightly lower than the previous ones in terms of energy absorption but show an improvement in terms of impacting forces. Although the cylinder shape shows a poorer performance when compared to the initial shape in the previous section, the genetic algorithm still reached similar results.

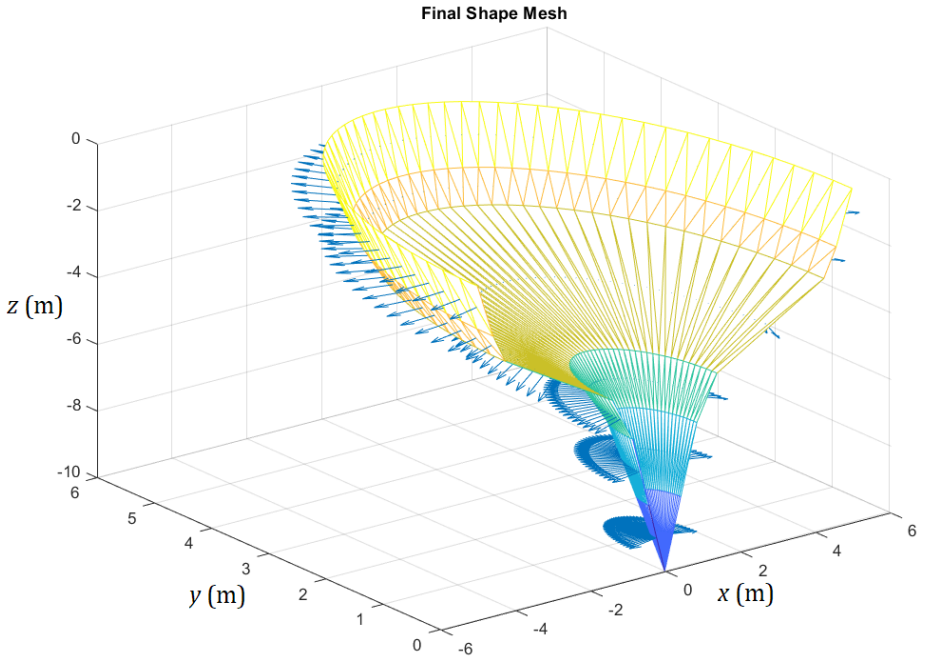

Figure 4.12. Final shape mesh for the cylinder case study.

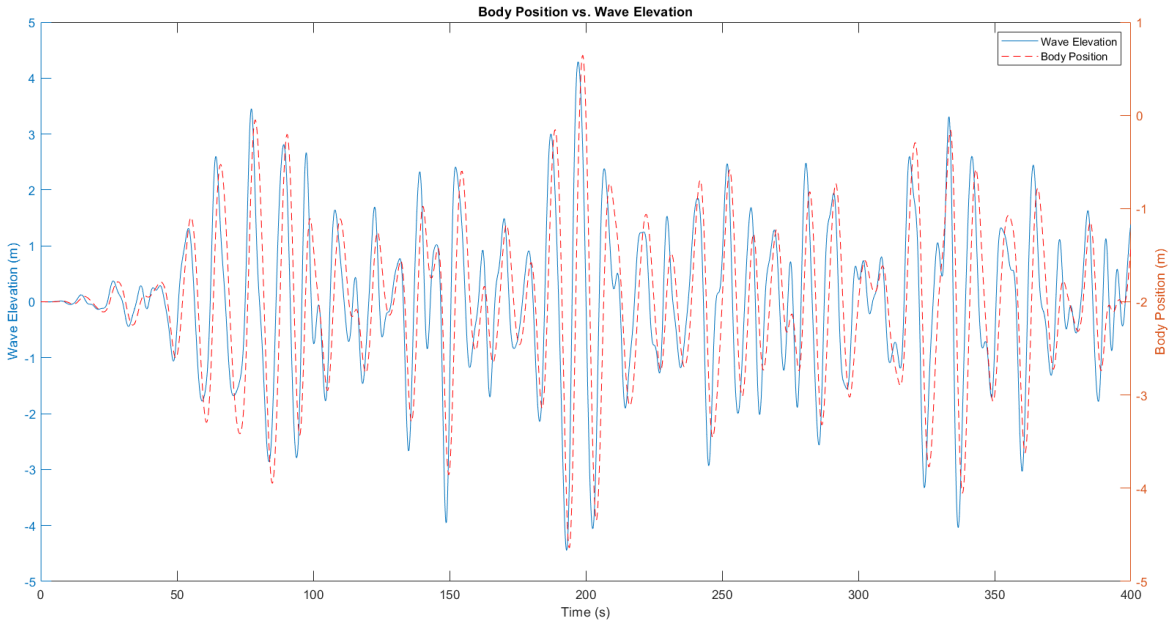

Figure 4.13. Body position of the resulting shape from the cylinder case study.

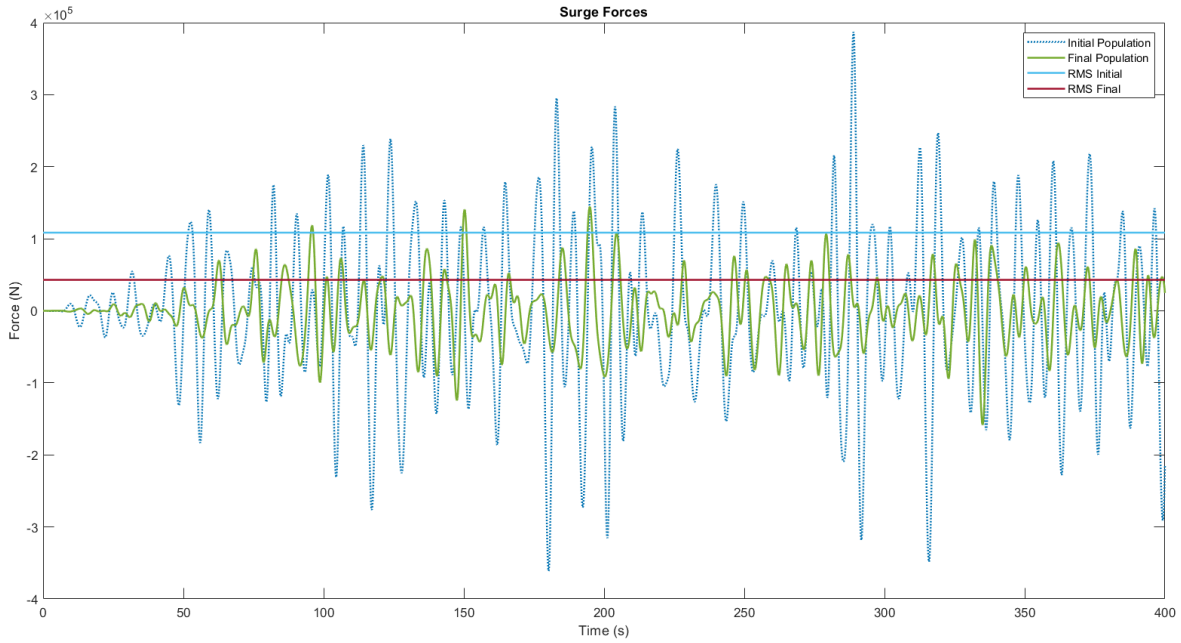

Figure 4.14. Surge total force result for the final shape from the cylinder case study.

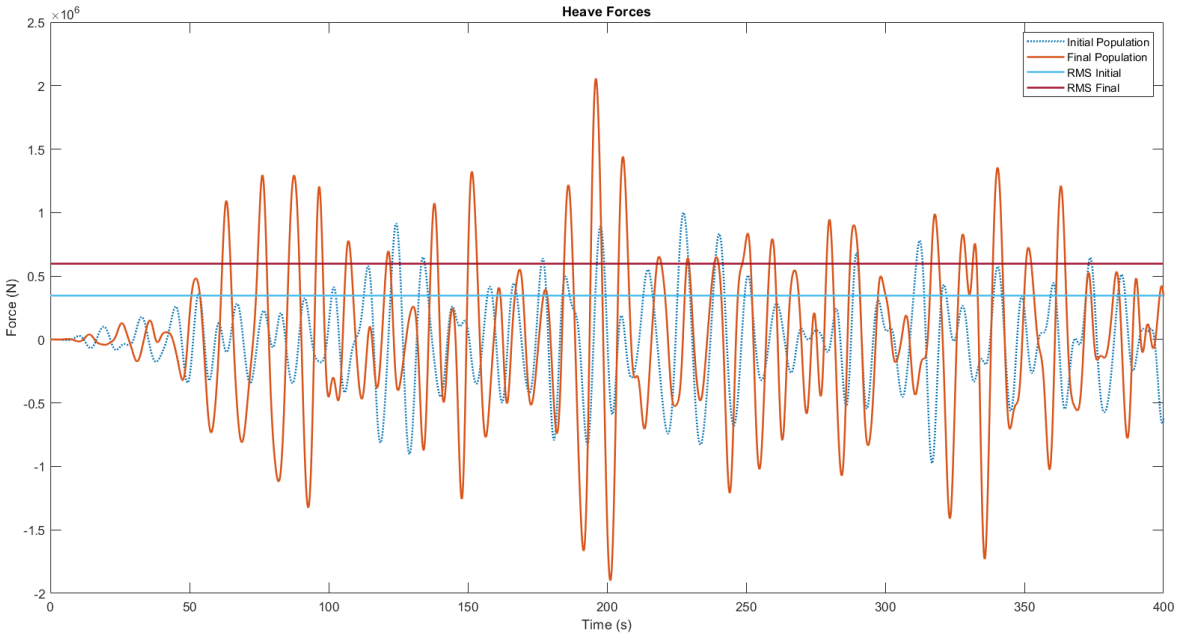

Figure 4.15. Heave total force result for the final shape from the cylinder case study.

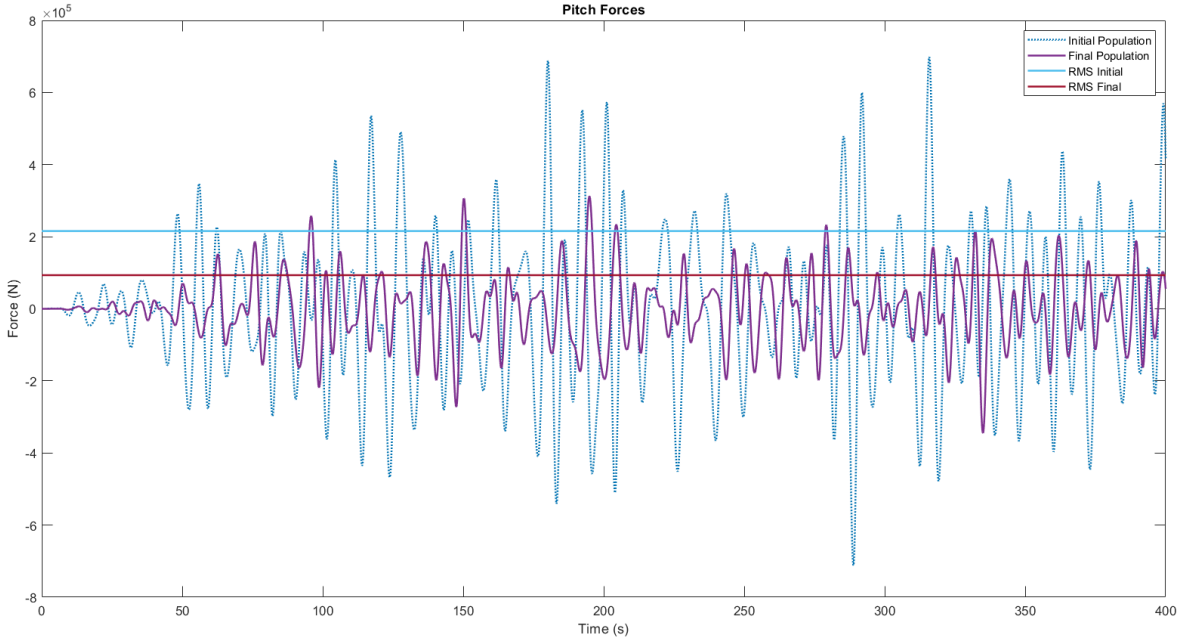

Figure 4.16. Pitch total force result for the final shape from the cylinder case study.

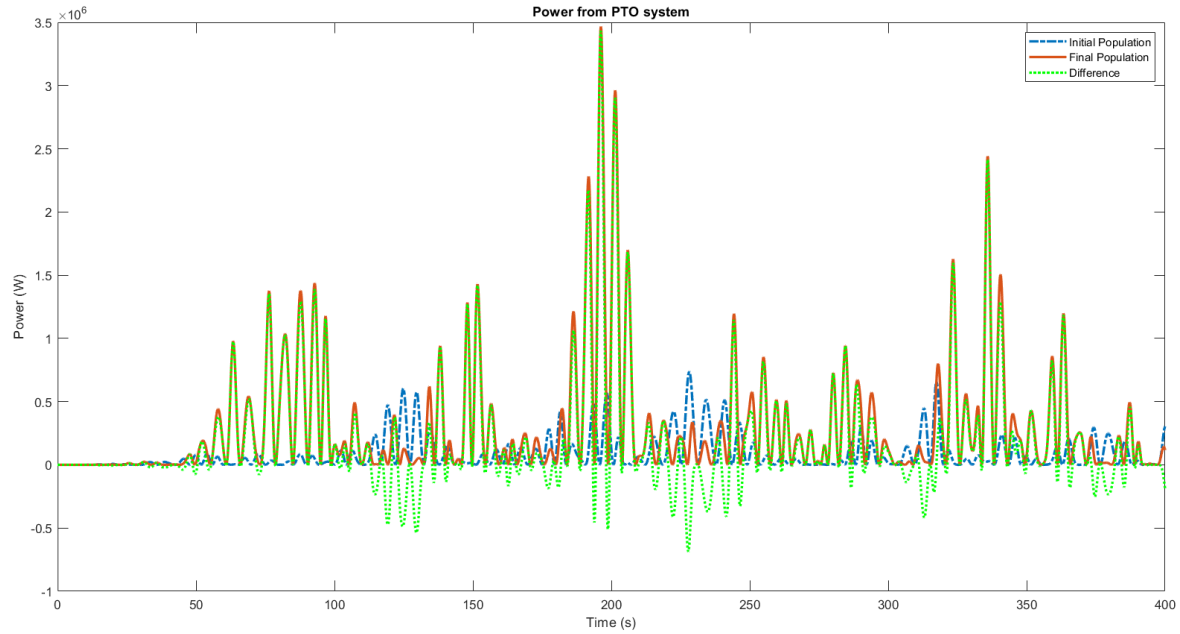

Figure 4.17. PTO absorbed power values for the final shape from the cylinder case study.

Table 4.4. Results from the optimisation process for the cylinder case study.

	SURGE FORCES (N)	HEAVE FORCES (N)	PITCH FORCES (N)	PTO POWER (W)	ENERGY (kWh)
CYLINDER SHAPE	1.08×10^5	3.46×10^5	2.16×10^5	1.53×10^5	17.01
FINAL SHAPE	4.30×10^4	5.97×10^5	9.33×10^4	5.45×10^5	60.60
VARIATION	60.19 %	72.54 %	56.81 %	256 %	256 %

The variation values in this algorithm run show a significant improvement from the cylinder shape, with decreased surge and pitch forces, and increased heave forces. In terms of energy, there was a remarkable increase of 256 %, due to the energy values of the cylinder being significantly lower than a shape as the one introduced to the first algorithm run. As shown in Table 4.4, the initial shape showed an energy value for that run of around 41 kWh, whereas the cylinder shape has a value of around 17 kWh.

4.2.3 *Average Wave Conditions*

After testing the impact of the first shape chosen, the results from the first optimisation run were tested under average wave conditions. The values for the wave parameters were obtained through the root mean square of a year long data series. The significant wave height value was 2.00 m, the peak period was 11.49 s, and the wave direction 302.84 °. Evaluating the device's performance in average wave conditions provides a more realistic assessment since it is the scenario that it will face most of the time. The results from the simulations are presented in Figure 4.18-Figure 4.22.

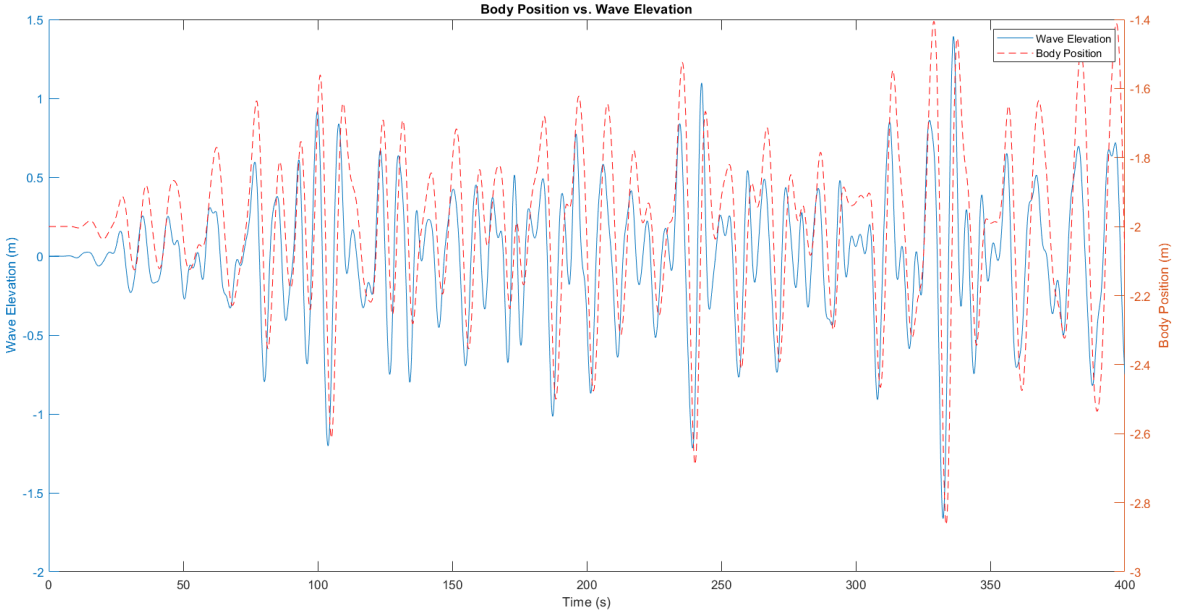

Figure 4.18. Body position of the resulting shape under average wave conditions.

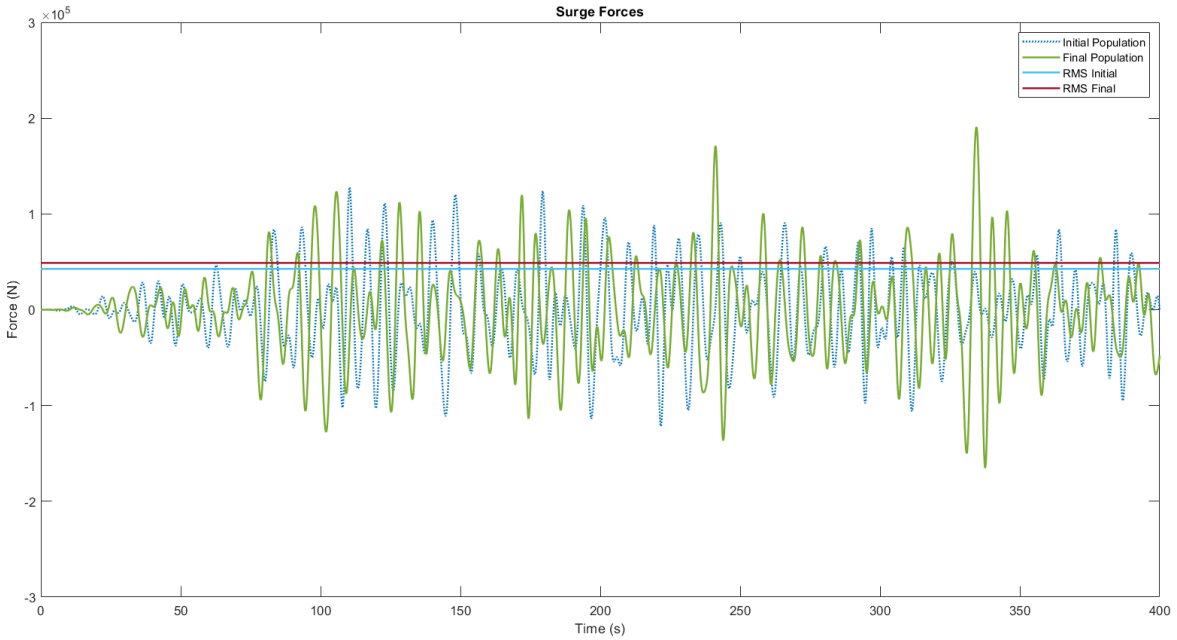

Figure 4.19. Surge total force result for the final shape under average wave conditions.

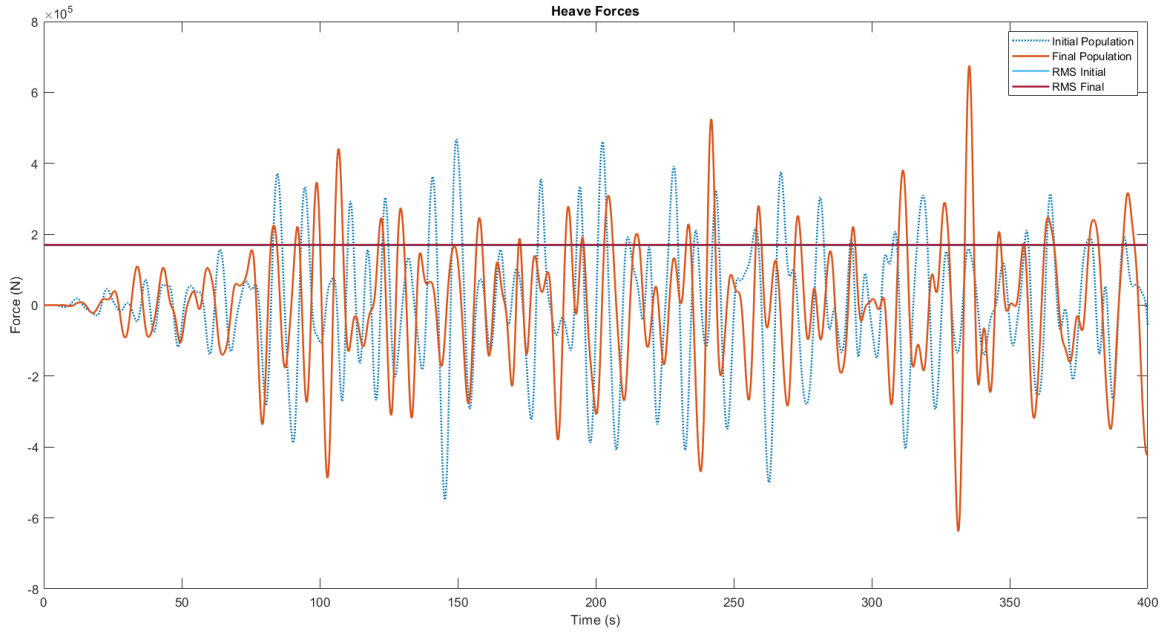

Figure 4.20. Heave total force result for the final shape under average wave conditions.

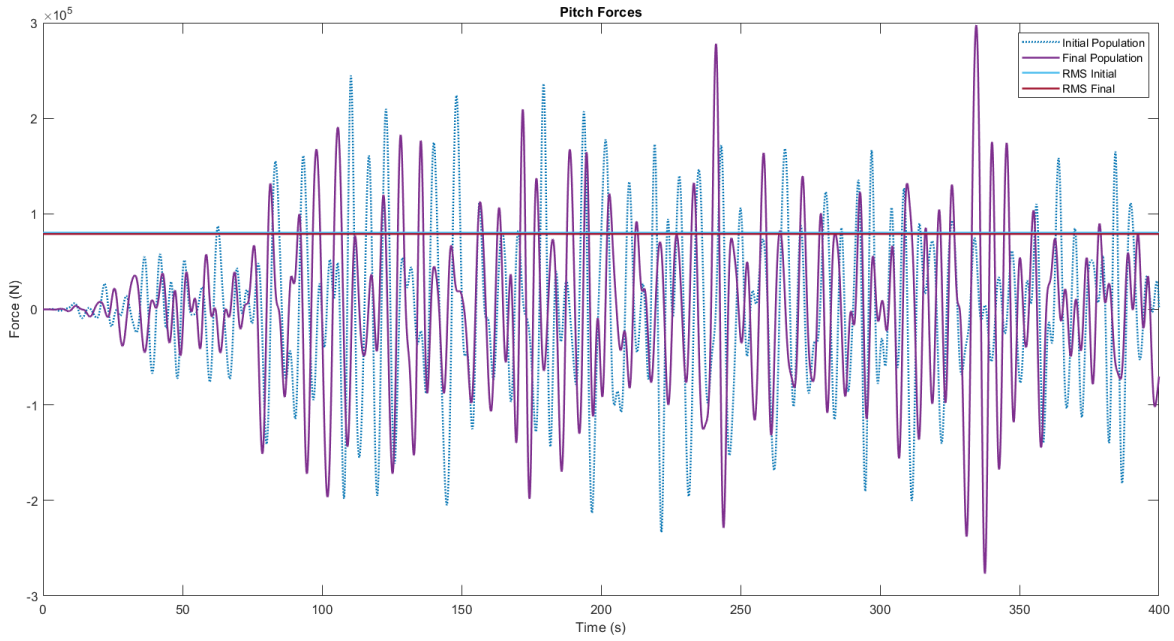

Figure 4.21. Pitch total force result for the final shape under average wave conditions.

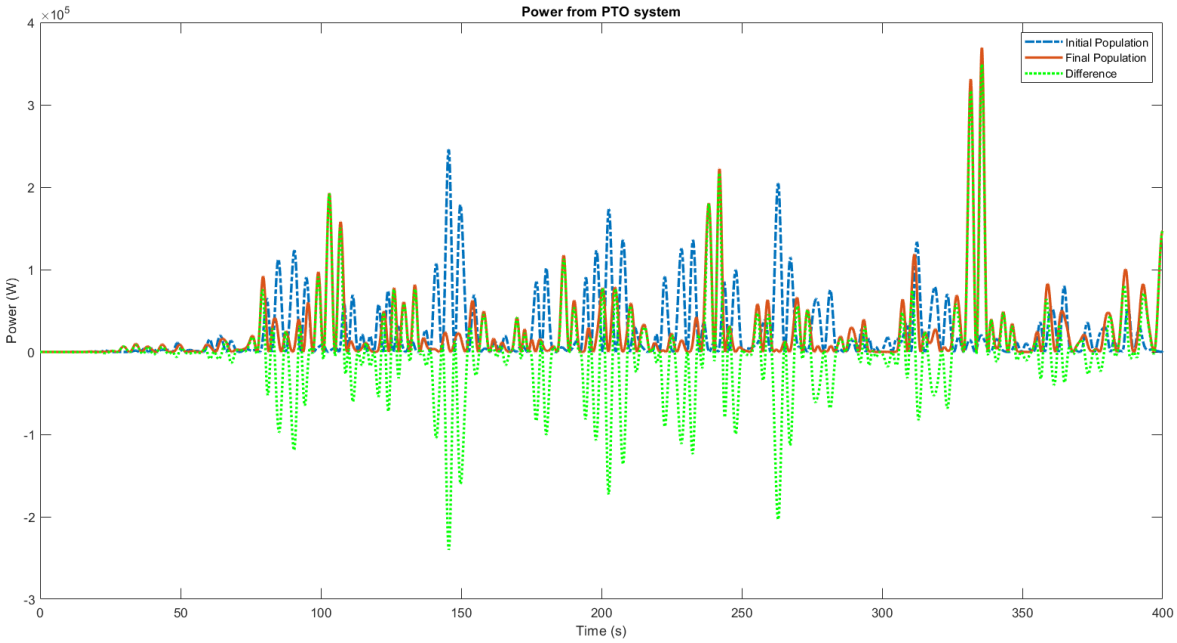

Figure 4.22. PTO absorbed power values for the final shape under average wave conditions.

Table 4.5 shows the values for surge, pitch, and heave total forces, as well as power from the PTO system and energy absorbed. Comparing these results with the extreme wave conditions, it is possible to verify a significantly lower difference, since the variation in energy values was 5 times lower. There is also an increased impact of the pitch and surge forces, and the difference in heave total force was small.

Table 4.5. Results from the optimisation process final shape, under average wave condition.

	SURGE FORCES (N)	HEAVE FORCES (N)	PITCH FORCES (N)	PTO POWER (W)	ENERGY (kWh)
INITIAL SHAPE	4.26×10^4	1.69×10^5	8.03×10^4	4.29×10^4	4.77
FINAL SHAPE	4.88×10^4	1.70×10^5	7.89×10^4	4.75×10^4	5.28
VARIATION	14.55 %	0.59 %	1.74 %	10.72 %	10.72 %

Comparing to previous simulations, the values for pitch and surge forces appear higher when in comparison to heave forces, which means that their expression in the movement

of the device is increased. This may lead to a lower value of extracted energy, since the considered PTO system extracts energy solely in heave.

4.3 RESOURCE EVALUATION

Evaluating the resulting shapes in terms of efficiency requires a comparison between the PTO absorbed power, P_{PTO}, and the wave power resource. It is possible to calculate the power density of the wave, P_{dens}, using the following equation [71]:

$$P_{dens} = \frac{\rho g^2}{64\pi} {H_s}^2 \alpha T_p \tag{12}$$

and then use the value of P_{wave}, which corresponds to the product of P_{dens} and the device width - 10 m - to calculate the efficiency, η, according to:

$$\eta = \frac{P_{PTO}}{P_{wave}}. \tag{13}$$

Calculating P_{dens} requires values for H_s and for T_p. For each of the sea states analysed, the wave power density value per unit length of wave front is presented in Table 4.6. The value for α was assumed to be 0.86 since the chosen type of wave spectrum was Pierson-Moskowitz [72].

Table 4.6. Parameter definition and results for wave power density.

	H_s (m)	T_p (s)	P_{dens} (kW/m)	P_{wave} (kW)
EXTREME WAVE CONDITION	4.78	10.82	104.09	1040.90
AVERAGE WAVE CONDITION	2.00	11.49	19.38	193.80

Using the values for absorbed PTO power for each of the simulations, provided in the tables from previous subsections, the efficiency values were calculated. The results are shown in Table 4.7.

Table 4.7. Efficiency values for the optimisation results.

	P_{PTO} (kW)	P_{wave} (kW)	η (%)
INITIAL SHAPE - EXTREME	371.00	1040.90	35.64
FINAL SHAPE - EXTREME	564.00	1040.90	54.18
INITIAL SHAPE - AVERAGE	42.90	193.80	22.14
FINAL SHAPE - AVERAGE	47.50	193.80	24.51
CYLINDER SHAPE	153.00	1040.90	14.70
FINAL SHAPE - CYLINDER	545.00	1040.90	52.36

There is a significant increase in efficiency from initial to final shapes under extreme wave conditions, both with a more conical initial shape and a cylinder, with the latter suffering a higher increase. Regarding the results under average wave conditions, the values are both low and with a small increase between initial and final shapes. This may be due to the high values for pitch and surge forces for these simulations as mentioned in the previous section. The difference between the cylinder case study initial and final shapes are significantly high because the results from the initial shape are poor when compared to the first case study, which did not use a cylinder as initial shape. When the final shapes from these two scenarios are compared, it is possible to observe a similar energy value.

Although the increase in efficiency is extremely positive, the values may differ when tested in real conditions since these simulations do not consider non-linear aspects of wave-structure interaction. Comparing the obtained values with other studies, it is possible to verify that the simulations with average wave conditions are the ones which approach the average values for efficiency for heaving wave energy converters, even though some may reach values as high as 51 % [73].

5

CONCLUSIONS AND FUTURE WORK

In this study, it was possible to develop an automated optimisation process to reach an optimal shape according to the main objectives defined. A validation process regarding the refinement of the used mesh was made, showing that a coarser mesh produces good enough results and the computational effort of a more refined mesh does not improve the solution significantly. The main optimisation process, which was designed to provide the key results of the study, was done under the harsher wave conditions for the chosen site. The results were also evaluated under average wave conditions. A second optimisation was made with an initial cylinder shape, to test if the results differed substantially when the initial shape is changed.

Finally, the results were compared to the available wave power to determine the efficiency of each shape. One of the main results from this study is the integration of the simulation and optimisation procedure in an automatic procedure using open-source software and MATLAB's genetic algorithm, requiring user interaction just in the initial parameter definition. It is also possible to adapt this process to other types of shapes and fitness functions, depending on the goals defined.

5.1 MAIN CONCLUSIONS

The optimisation process produced satisfying results regarding absorbed power, however, it was not possible to reduce the effect of surge and pitch forces as intended, in order to reduce possible stresses on the device and improve its robustness. Nonetheless, the absorbed energy was increased under the same wave conditions for the final shapes. This increase was lower for the average wave conditions, which may be due to the fact that the final shape was tuned to the harsher wave conditions, and so an optimisation process dedicated solely to these conditions should be considered.

The use of a different initial shape did not show a great significance in terms of results, since the final shape from the optimisation process starting with a cylinder reached similar values in terms of absorbed power to those obtained for a more conical initial shape.

The efficiency values obtained may be higher than expected since nonlinear effects aren't considered. The optimisation process was successfully automated and implemented, allowing it to be used in other types of studies.

This work was also presented at the 1st International Conference on Machine Design, on the 9th of September of 2021. Besides providing the means to share the developed work, it also allowed other peers to make suggestions and comment on it.

5.2 FUTURE WORK

Future developments should include testing different deployment sites to test the dependence of the device performance on the chosen location. A prototype should also be built to be tested in a wave tank and validate the results given by the models. An optimisation scenario exclusively for average wave conditions should also analysed, since using the results from other wave conditions revealed poor performances.

In terms of the optimisation process, different objective functions could be tested, as well as a multi-objective optimisation, to broaden the scope of the built process.

BIBLIOGRAPHY

[1] D. Larcher and J.-M. Tarascon. "Towards greener and more sustainable batteries for electrical energy storage." In: *Nature Chemistry* 7.1 (2015). cited By 3653, pp. 19–29. DOI: 10.1038/nchem.2085. URL: https://www.scopus.com/inward/record.uri?eid=2-s2.0-84924528297&doi=10.1038\%2fnchem.2085&partnerID=40&md5=afe6169101aa213230a3355e9e6381fa.

[2] Adriana Ressurreição, James Gibbons, Tomaz Ponce Dentinho, Michel Kaiser, Ricardo S. Santos, and Gareth Edwards-Jones. "Economic valuation of species loss in the open sea." In: *Ecological Economics* 70.4 (2011), pp. 729–739. ISSN: 0921-8009. DOI: https://doi.org/10.1016/j.ecolecon.2010.11.009. URL: https://www.sciencedirect.com/science/article/pii/S0921800910004623.

[3] Mehmet Melikoglu. "Current status and future of ocean energy sources: A global review." In: *Ocean Engineering* 148 (2018), pp. 563–573. ISSN: 00298018. DOI: 10.1016/j.oceaneng.2017.11.045.

[4] N. Khan, A. Kalair, N. Abas, and A. Haider. "Review of ocean tidal, wave and thermal energy technologies." In: *Renewable and Sustainable Energy Reviews* 72 (2017), pp. 590–604. ISSN: 18790690. DOI: 10.1016/j.rser.2017.01.079.

[5] Johannes Falnes. "A review of wave-energy extraction." In: *Marine Structures* 20.4 (2007), pp. 185–201. ISSN: 09518339. DOI: 10.1016/j.marstruc.2007.09.001.

[6] P. Mota and J. P. Pinto. "Wave energy potential along the western Portuguese coast." In: *Renewable Energy* 71 (2014), pp. 8–17. ISSN: 09601481. DOI: 10.1016/j.renene.2014.02.039.

[7] European Marine Energy Centre (EMEC). *Wave devices*. URL: http://www.emec.org.uk/marine-energy/wave-devices/ (visited on 03/15/2021).

[8] European Marine Energy Centre (EMEC). *Wave developers*. URL: http://www.emec.org.uk/marine-energy/wave-developers/ (visited on 03/15/2021).

[9] D. Clemente, P. Rosa-Santos, and F. Taveira-Pinto. "On the potential synergies and applications of wave energy converters: A review." In: *Renewable and Sustainable Energy Reviews* 135 (2021). ISSN: 18790690. DOI: 10.1016/j.rser.2020.110162.

[10] António F.de O. Falcão. "Wave energy utilization: A review of the technologies." In: *Renewable and Sustainable Energy Reviews* 14.3 (2010), pp. 899–918. ISSN: 13640321. DOI: 10.1016/j.rser.2009.11.003.

[11] Malin Göteman, Marianna Giassi, Jens Engström, and Jan Isberg. "Advances and Challenges in Wave Energy Park Optimization—A Review." In: *Frontiers in Energy Research* 8 (2020). ISSN: 2296598X. DOI: 10.3389/fenrg.2020.00026.

[12] A. Garcia-Teruel and D. I.M. Forehand. "A review of geometry optimisation of wave energy converters." In: *Renewable and Sustainable Energy Reviews* 139 (2021). ISSN: 18790690. DOI: 10.1016/j.rser.2020.110593.

[13] Juan P. Ortiz, Helen Bailey, Bradley Buckham, and Curran Crawford. "Surrogate based design of a mooring system for a self-reacting point absorber." In: *Proceedings of the International Offshore and Polar Engineering Conference*. Vol. 2015-Janua. International Society of Offshore and Polar Engineers, 2015, pp. 936–943. ISBN: 9781880653890.

[14] Jonas Thomsen, Francesco Ferri, Jens Kofoed, and Kevin Black. "Cost Optimization of Mooring Solutions for Large Floating Wave Energy Converters." In: *Energies* 11.1 (2018), p. 159. ISSN: 1996-1073. DOI: 10.3390/en11010159. URL: http://www.mdpi.com/1996-1073/11/1/159.

[15] Nestor V. Queipo, Raphael T. Haftka, Wei Shyy, Tushar Goel, Rajkumar Vaidyanathan, and P. Kevin Tucker. "Surrogate-based analysis and optimization." In: *Progress in Aerospace Sciences* 41.1 (2005), pp. 1–28. ISSN: 03760421. DOI: 10.1016/j.paerosci.2005.02.001. URL: https://linkinghub.elsevier.com/retrieve/pii/S0376042105000102.

[16] Pau Ruiz, Vincenzo Nava, Mathew Topper, Pablo Minguela, Francesco Ferri, and Jens Kofoed. "Layout Optimisation of Wave Energy Converter Arrays." In: *Energies* 10.9 (2017), p. 1262. ISSN: 1996-1073. DOI: 10.3390/en10091262. URL: http://www.mdpi.com/1996-1073/10/9/1262.

[17] Chris Sharp and Bryony DuPont. "Wave energy converter array optimization: A genetic algorithm approach and minimum separation distance study." In: *Ocean Engineering* 163 (2018), pp. 148–156. ISSN: 00298018. DOI: 10.1016/j.oceaneng.2018.05.071.

[18] Marianna Giassi, Malin Göteman, Simon Thomas, Jens Engström, Mikael Eriksson, and Jan Isberg. "Multi-Parameter Optimization of Hybrid Arrays of Point Absorber Wave Energy Converters." In: *Proceedings of the 12th European Wave and Tidal Energy Conference*. 2017.

[19] Arthur Pecher and Jens Peter Kofoed, eds. *Handbook of Ocean Wave Energy*. Vol. 7. Ocean Engineering & Oceanography. Cham: Springer International Publishing, 2017. ISBN: 978-3-319-39888-4. DOI: 10.1007/978-3-319-39889-1. URL: http://link.springer.com/10.1007/978-3-319-39889-1.

[20] Milad Shadman, Segen F. Estefen, Claudio A. Rodriguez, and Izabel C.M. Nogueira. "A geometrical optimization method applied to a heaving point absorber wave energy converter." In: *Renewable Energy* 115 (2018), pp. 533–546. ISSN: 18790682. DOI: 10.1016/j.renene.2017.08.055.

[21] Elie Al Shami, Ran Zhang, and Xu Wang. "Point absorber wave energy harvesters: A review of recent developments." In: *Energies* 12.1 (2019). ISSN: 19961073. DOI: 10.3390/en12010047.

[22] Iraide López, Jon Andreu, Salvador Ceballos, Iñigo Martínez De Alegría, and Iñigo Kortabarria. "Review of wave energy technologies and the necessary power-equipment." In: *Renewable and Sustainable Energy Reviews* 27 (2013), pp. 413–434. ISSN: 13640321. DOI: 10.1016/j.rser.2013.07.009. URL: https://linkinghub.elsevier.com/retrieve/pii/S1364032113004541.

[23] Erik Lejerskog, Cecilia Boström, Ling Hai, Rafael Waters, and Mats Leijon. "Experimental results on power absorption from a wave energy converter at the Lysekil wave energy research site." In: *Renewable Energy* 77 (2015), pp. 9–14. ISSN: 18790682. DOI: 10.1016/j.renene.2014.11.050.

[24] Zia Saadatnia, Ehsan Asadi, Hassan Askari, Ebrahim Esmailzadeh, and Hani E. Naguib. "A heaving point absorber-based triboelectric-electromagnetic wave energy harvester: An efficient approach toward blue energy." In: *International Journal of Energy Research* 42.7 (2018), pp. 2431–2447. ISSN: 1099114X. DOI: 10.1002/er.4024.

[25] Tunde Aderinto and Hua Li. "Conceptual design and simulation of a self-adjustable heaving point absorber based wave energy converter." In: *Energies* 13.8 (2020). ISSN: 19961073. DOI: 10.3390/en13081997.

[26] Vincenzo Piscopo, Guido Benassai, Renata Della Morte, and Antonio Scamardella. "Cost-based design and selection of point absorber devices for the Mediterranean Sea." In: *Energies* 11.4 (2018). ISSN: 19961073. DOI: 10.3390/en11040946.

[27] Pablo Ropero-Giralda, Alejandro J.C. Crespo, Bonaventura Tagliafierro, Corrado Altomare, José M. Domínguez, Moncho Gómez-Gesteira, and Giacomo Viccione. "Efficiency and survivability analysis of a point-absorber wave energy converter using DualSPHysics." In: *Renewable Energy* 162 (2020), pp. 1763–1776. ISSN: 18790682. DOI: 10.1016/j.renene.2020.10.012.

[28] Jeremiah Pastor and Yucheng Liu. "Frequency and time domain modeling and power output for a heaving point absorber wave energy converter." In: *International Journal of Energy and Environmental Engineering* 5.2-3 (2014), pp. 1–13. ISSN: 22516832. DOI: 10.1007/s40095-014-0101-9.

[29] Markel Penalba, Thomas Kelly, and John Ringwood. "Using NEMOH for Modelling Wave Energy Converters: A Comparative Study with WAMIT." In: (2017). URL: http://eprints.maynoothuniversity.ie/12466/.

[30] Wendt et al. "Ocean Energy Systems Wave Energy Modelling Task: Modelling, Verification and Validation of Wave Energy Converters." In: *Journal of Marine Science and Engineering* 7.11 (2019), p. 379. ISSN: 2077-1312. DOI: 10.3390/jmse7110379. URL: https://www.mdpi.com/2077-1312/7/11/379.

[31] Aurélien Babarit and Gérard Delhommeau. "Theoretical and numerical aspects of the open source BEM solver NEMOH." In: *11th European Wave and Tidal Energy Conference (EWTEC2015)*. Proceedings of the 11th European Wave and Tidal Energy Conference. Nantes, France, Sept. 2015. URL: https://hal.archives-ouvertes.fr/hal-01198800.

[32] Inc WAMIT. *WAMIT User Manual - Version 7.3*. Massachusetts, USA, 2019.

[33] Ossama Abdelkhalik, Ryan G. Coe, Giorgio Bacelli, and David G. Wilson. "WEC geometry optimization with advanced control." In: *Proceedings of the International Conference on Offshore Mechanics and Arctic Engineering - OMAE*. Vol. 10. American Society of Mechanical Engineers (ASME), 2017. ISBN: 9780791857786. DOI: 10.1115/OMAE2017-61917.

[34] Rezvan Alamian, Rouzbeh Shafaghat, and Mohammad Reza Safaei. "Multi-objective optimization of a pitch point absorber wave energy converter." In: *Water (Switzerland)* 11.5 (2019). ISSN: 20734441. DOI: 10.3390/w11050969.

[35] Y. Wei, J. J. Barradas-Berglind, Z. Yu, M. van Rooij, W. A. Prins, B. Jayawardhana, and A. I. Vakis. "Frequency-domain hydrodynamic modelling of dense and sparse arrays of wave energy converters." In: *Renewable Energy* 135 (2019), pp. 775–788. ISSN: 18790682. DOI: 10.1016/j.renene.2018.12.022.

[36] Soheil Esmaeilzadeh and Mohammad Reza Alam. "Shape optimization of wave energy converters for broadband directional incident waves." In: *Ocean Engineering* 174 (2019), pp. 186–200. ISSN: 00298018. DOI: 10.1016/j.oceaneng.2019.01.029. arXiv: 1805.08294.

[37] A. P. McCabe, G. A. Aggidis, and M. B. Widden. "Optimizing the shape of a surge-and-pitch wave energy collector using a genetic algorithm." In: *Renewable Energy* 35.12 (2010), pp. 2767–2775. ISSN: 09601481. DOI: 10.1016/j.renene.2010.04.029.

[38] Linnea Sjökvist, Remya Krishna, Magnus Rahm, Valeria Castellucci, Hagnestål Anders, and Mats Leijon. "On the Optimization of Point Absorber Buoys." In: *Journal of Marine Science and Engineering* 2.2 (2014), pp. 477–492. ISSN: 2077-1312. DOI: 10.3390/jmse2020477. URL: http://www.mdpi.com/2077-1312/2/2/477.

[39] António F.O. Falcão, João C.C. Henriques, and José J. Cândido. "Dynamics and optimization of the OWC spar buoy wave energy converter." In: *Renewable Energy* 48 (2012), pp. 369–381. ISSN: 09601481. DOI: 10.1016/j.renene.2012.05.009.

[40] Yuzhu Li, Heather Peng, Wei Qiu, Brian Lundrigan, and Tim Gardiner. "Hydrodynamic analysis and optimization of a hinged type wave energy converter." In: *Proceedings of the International Conference on Offshore Mechanics and Arctic Engineering - OMAE*. Vol. 6. American Society of Mechanical Engineers (ASME), 2016. ISBN: 9780791849972. DOI: 10.1115/OMAE2016-54911.

[41] Jennifer van Rij, Yi Hsiang Yu, Yi Guo, and Ryan G. Coe. "A wave energy converter design load case study." In: *Journal of Marine Science and Engineering* 7.8 (2019). ISSN: 20771312. DOI: 10.3390/jmse7080250.

[42] Brad Stappenbelt and Paul Cooper. "Optimisation of a floating oscillating water column wave energy converter." In: *Proceedings of the International Offshore and Polar Engineering Conference*. Vol. 1. 2010, pp. 788–795. ISBN: 9781880653777.

[43] Jianguo Dong, Jingwei Gao, Peng Zheng, and Yuanchao Zhang. "Numerical simulation and structural optimization based on an elliptical and cylindrical raft wave energy conversion device." In: *Journal of Renewable and Sustainable Energy* 10.6 (2018), p. 064702. ISSN: 19417012. DOI: 10.1063/1.5042269. URL: http://aip.scitation.org/doi/10.1063/1.5042269.

[44] Xueyu Ji, Elie Al Shami, Jason Monty, and Xu Wang. "Modelling of linear and non-linear two-body wave energy converters under regular and irregular wave conditions." In: *Renewable Energy* 147 (2020), pp. 487–501. ISSN: 18790682. DOI: 10.1016/j.renene.2019.09.010.

[45] Yong Ma, Shan Ai, Lele Yang, Aiming Zhang, Sen Liu, and Binghao Zhou. "Hydrodynamic performance of a pitching float wave energy converter." In: *Energies* 13.7 (2020). ISSN: 19961073. DOI: 10.3390/en13071801.

[46] Srinivasan Chandrasekaran and V. V.S. Sricharan. "Numerical analysis of a new multi-body floating wave energy converter with a linear power take-off system." In: *Renewable Energy* 159 (2020), pp. 250–271. ISSN: 18790682. DOI: 10.1016/j.renene.2020.06.007.

[47] Davy Pardonner, Nathan Tom, and Yi Guo. "Numerical model development of a variable-geometry attenuator wave energy converter." In: *Proceedings of the International Conference on Offshore Mechanics and Arctic Engineering - OMAE*. Vol. 9. American Society of Mechanical Engineers (ASME), 2020. ISBN: 97807918844l6. DOI: 10.1115/omae2020-19054.

[48] Mohammad Hayati, Amir H. Nikseresht, and Ali Taherian Haghighi. "Sequential optimization of the geometrical parameters of an OWC device based on the specific wave characteristics." In: *Renewable Energy* 161 (2020), pp. 386–394. ISSN: 18790682. DOI: 10.1016/j.renene.2020.07.073.

[49] Rodrigo C. Lisboa, Paulo R.F. Teixeira, Fernando R. Torres, and Eric Didier. "Numerical evaluation of the power output of an oscillating water column wave energy converter installed in the southern Brazilian coast." In: *Energy* 162 (2018), pp. 1115–1124. ISSN: 03605442. DOI: 10.1016/j.energy.2018.08.079.

[50] G. Ozdamar and Y. Pekbey. "Numerical optimization of the blade surface geometry in a wave turbine system." In: *Acta Physica Polonica A*. Vol. 134. 1. Polish Academy of Sciences, 2018, pp. 150–152. DOI: 10.12693/APhysPolA.134.150.

[51] Xiaoxia Zhang, Qiang Zeng, and Zhen Liu. "Hydrodynamic performance of rectangular heaving buoys for an integrated floating breakwater." In: *Journal of Marine Science and Engineering* 7.8 (2019). ISSN: 20771312. DOI: 10.3390/jmse7080239.

[52] B. Bouali and S. Larbi. "Contribution to the geometry optimization of an oscillating water column wave energy converter." In: *Energy Procedia*. Vol. 36. Elsevier Ltd, 2013, pp. 565–573. DOI: 10.1016/j.egypro.2013.07.065.

[53] William Finnegan and Jamie Goggins. "Numerical simulation of linear water waves and wavestructure interaction." In: *Ocean Engineering* 43 (2012), pp. 23–31. ISSN: 00298018. DOI: 10.1016/j.oceaneng.2012.01.002.

[54] Majid A. Bhinder, Clive G. Mingham, Derek M. Causon, Mohammad T. Rahmati, George A. Aggidis, and Robert V. Chaplin. "A joint numerical and experimental study of asurging point absorbing wave energy converter (WRASPA)." In: *Proceedings of the International Conference on Offshore Mechanics and Arctic Engineering - OMAE*. Vol. 4. PART B. 2009, pp. 869–875. ISBN: 9780791843444. DOI: 10.1115/OMAE2009-79392.

[55] Farrokh Mahnamfar, Abdüsselam Altunkaynak, and Yasin Abdollahzadehmoradi. "Comparison of Experimental and Numerical Model Results of Oscillating Water Column System Under Regular Wave Conditions." In: *Iranian Journal of Science and Technology - Transactions of Civil Engineering* 44.1 (2020), pp. 299–315. ISSN: 23641843. DOI: 10.1007/s40996-019-00259-x.

[56] Anna Garcia-Teruel, Bryony DuPont, and David I.M. Forehand. "Hull geometry optimisation of wave energy converters: On the choice of the optimisation algorithm and the geometry definition." In: *Applied Energy* 280 (2020), p. 115952. ISSN: 03062619. DOI: 10.1016/j.apenergy.2020.115952.

[57] V. Piscopo, G. Benassai, L. Cozzolino, R. Della Morte, and A. Scamardella. "A new optimization procedure of heaving point absorber hydrodynamic performances." In: *Ocean Engineering* 116 (2016), pp. 242–259. ISSN: 00298018. DOI: 10.1016/j.oceaneng.2016.03.004.

[58] A. P. McCabe. "Constrained optimization of the shape of a wave energy collector by genetic algorithm." In: *Renewable Energy* 51 (2013), pp. 274–284. ISSN: 09601481. DOI: 10.1016/j.renene.2012.09.054.

[59] Jean Christophe Gilloteaux and John Ringwood. "Control-informed geometric optimisation of wave energy converters." In: *IFAC Proceedings Volumes (IFAC-PapersOnline)*. Vol. 43. 20. IFAC Secretariat, 2010, pp. 366–371. ISBN: 9783902661883. DOI: 10.3182/20100915-3-DE-3008.00072.

[60] R. P.F. Gomes, J. C.C. Henriques, L. M.C. Gato, and A. F.O. Falcão. "Hydrodynamic optimization of an axisymmetric floating oscillating water column for wave energy conversion." In: *Renewable Energy* 44 (2012), pp. 328–339. ISSN: 09601481. DOI: 10.1016/j.renene.2012.01.105.

[61] Erin E. Bachynski, Yin Lu Young, and Ronald W. Yeung. "Analysis and optimization of a tethered wave energy converter in irregular waves." In: *Renewable Energy* 48 (2012), pp. 133–145. ISSN: 0960-1481. DOI: 10.1016/J.RENENE.2012.04.044.

[62] Matt Folley. "The Wave Energy Resource." In: *Handbook of Ocean Wave Energy*. Ed. by Arthur Pecher and Jens Peter Kofoed. Cham: Springer International Publishing, 2017, pp. 43–79. ISBN: 978-3-319-39889-1. DOI: 10.1007/978-3-319-39889-1_3. URL: https://doi.org/10.1007/978-3-319-39889-1_3.

[63] M. Alves. "Chapter 2 - Frequency-Domain Models." In: *Numerical Modelling of Wave Energy Converters*. Ed. by Matt Folley. Academic Press, 2016, pp. 11–30. ISBN: 978-0-12-803210-7. DOI: https://doi.org/10.1016/B978-0-12-803210-7.00002-5. URL: https://www.sciencedirect.com/science/article/pii/B9780128032107000025.

[64] NREL & Sandia. *WEC-Sim Documentation*. URL: https://wec-sim.github.io/WEC-Sim/master/index.html.

[65] *Marine energy - Wave, tidal and other water current converters - Part 2: Marine energy systems - Design requirements*. en. Standard IEC TS 62600-2:2019. Geneva, CH: International Electrotechnical Commission, 2019. URL: https://webstore.iec.ch/publication/62399.

[66] Yi-Hsiang Yu, Kelley Ruehl, Jennifer Van Rij, Nathan Tom, Dominic Forbush, David Ogden, Adam Keester, and Jorge Leon. *WEC-Sim v4.3*. Version v4.3. 2021. DOI: 10.5281/zenodo.5122959. URL: https://doi.org/10.5281/zenodo.5122959.

[67] CMEMS. *Global Ocean Waves Analysis and Forecast*. URL: https://resources.marine.copernicus.eu/product-detail/GLOBAL_ANALYSIS_FORECAST_WAV_001_027/INFORMATION.

[68] Simon P. Neill and M. Reza Hashemi. "Chapter 5 - Wave Energy." In: *Fundamentals of Ocean Renewable Energy*. Ed. by Simon P. Neill and M. Reza Hashemi. E-Business Solutions. Academic Press, 2018, pp. 107–140. ISBN: 978-0-12-810448-4. DOI: https://doi.org/10.1016/B978-0-12-810448-4.00005-7. URL: https://www.sciencedirect.com/science/article/pii/B9780128104484000057.

[69] J.-R. Bidlot, D.J. Holmes, P.A. Wittmann, R. Lalbeharry, and H.S. Chen. "Intercomparison of the performance of operational ocean wave forecasting systems with buoy data." In: *Weather and Forecasting* 17.2 (2002). cited By 182, pp. 287–310. DOI: 10.1175/1520-0434(2002)017<0287:IOTPOO>2.0.CO;2. URL: https://www.scopus.com/inward/record.uri?eid=2-s2.0-0036552804&doi=10.1175\%2f1520-0434\%282002\%29017\%3c0287\%3aIOTPOO\%3e2.0.CO\%3b2&partnerID=40&md5=286444e000ec489d826fd105b10b9fc9.

[70] MathWorks. *MATLAB Global Optimization Toolbox: User's Guide*. Mathworks. Natick, Massachusetts, 2021.

[71] Nicolas Guillou. "Estimating wave energy flux from significant wave height and peak period." In: *Renewable Energy* 155 (2020), pp. 1383–1393. ISSN: 0960-1481. DOI: https://doi.org/10.1016/j.renene.2020.03.124. URL: https://www.sciencedirect.com/science/article/pii/S0960148120304560.

[72] Felice Arena, Valentina Laface, Giovanni Malara, Alessandra Romolo, Antonino Viviano, Vincenzo Fiamma, Gianmaria Sannino, and Adriana Carillo. "Wave climate analysis for the design of wave energy harvesters in the Mediterranean Sea." In: *Renewable Energy* 77 (2015), pp. 125–141. ISSN: 0960-1481. DOI: https://doi.org/10.1016/j.renene.2014.12.002. URL: https://www.sciencedirect.com/science/article/pii/S0960148114008283.

[73] Tunde Aderinto and Hua Li. "Review on power performance and efficiency of wave energy converters." In: *Energies* 12.22 (2019). ISSN: 19961073. DOI: 10.3390/en12224329.

COLOPHON

This document was typeset using the typographical look-and-feel `classicthesis` developed by André Miede. The style was inspired by Robert Bringhurst's seminal book on typography "*The Elements of Typographic Style*". `classicthesis` is available for both LaTeX and LyX.

Final Version as of December 15, 2021 (`version 2.0`).

APPENDIX A - CHANGES TO MESH GENERATION FUNCTION

```
% Warning : z(i) must be greater than z(i+1)
%
% Copyright Ecole Centrale de Nantes 2014
% Licensed under the Apache License, Version 2.0
% Written by A. Babarit, LHEEA Lab.
%
function [Mass,Inertia,KH,XB,YB,ZB]=axiMeshAutom(r,z,n,ntheta,nomrep,zG,nfobj)
rho=1025;
g=9.81;
status=close('all');
theta=[0.:pi/(ntheta-1):pi];
nx=0;
% Calcul des sommets du maillage
for j=1:ntheta
    for i=1:n
        nx=nx+1;
        x(nx)=r(i)*cos(theta(j));
        y(nx)=r(i)*sin(theta(j));
        z(nx)=z(i);
    end;
end;
% Calcul des facettes
nf=0;
for i=1:n-1
    for j=1:ntheta-1
        nf=nf+1;
        NN(1,nf)=i+n*(j-1);
        NN(2,nf)=i+1+n*(j-1);
        NN(3,nf)=i+1+n*j;
        NN(4,nf)=i+n*j;
    end;
end;
```

```
% Affichage de la description du maillage
nftri=0;
for i=1:nf
    nftri=nftri+1;
    tri(nftri,:)=[NN(1,i) NN(2,i) NN(3,i)];
    nftri=nftri+1;
    tri(nftri,:)=[NN(1,i) NN(3,i) NN(4,i)];
end;
figure;
trimesh(tri,x,y,z,[zeros(nx,1)]);
title('Characteristics of the discretisation');
fprintf('\n --> Number of nodes             : %g',nx);
fprintf('\n --> Number of panels (max 2000) : %g \n',nf);
system(['mkdir ',nomrep]);
system(['mkdir ',nomrep,filesep,'mesh']);
system(['mkdir ',nomrep,filesep,'results']);
% Creation des fichiers de calcul du maillage
fid=fopen('Mesh.cal','w');
fprintf(fid,'axisym \n',1);
fprintf(fid,'1 \n 0. 0. \n ');
fprintf(fid,'%f %f %f \n',[0. 0. zG]);
fprintf(fid,'%g \n 2 \n 0. \n 1.\n',nfobj);
fprintf(fid,'%f \n %f \n',[rho g]);
status=fclose(fid);
fid=fopen('ID.dat','w');
fprintf(fid,['% g \n',nomrep,' \n'],length(nomrep));
status=fclose(fid);
fid=fopen([nomrep,filesep,'mesh',filesep,'axisym'],'w');
fprintf(fid,'%g \n',nx);
fprintf(fid,'%g \n',nf);
for i=1:nx
    fprintf(fid,'%E %E %E \n',[x(i) y(i) z(i)]);
end;
for i=1:nf
    fprintf(fid,'%g %g %g %g \n',NN(:,i)');
end;
status=fclose(fid);
```

```
% Raffinement automatique du maillage et calculs hydrostatiques
l = isunix;
if l == 1
    system('mesh >Mesh.log');
else
    system('.\Mesh\Mesh.exe >Mesh\Mesh.log');
end
% Visualisation du maillage
clear x y z NN nx nf nftri tri u v w;
fid=fopen([nomrep,filesep,'mesh',filesep,'axisym.tec'],'r');
ligne=fscanf(fid,'%s',2);
nx=fscanf(fid,'%g',1);
ligne=fscanf(fid,'%s',2);
nf=fscanf(fid,'%g',1);
ligne=fgetl(fid);
fprintf('\n Characteristics of the mesh for Nemoh \n');
fprintf('\n --> Number of nodes : %g',nx);
fprintf('\n --> Number of panels : %g\n \n',nf);
for i=1:nx
    ligne=fscanf(fid,'%f',6);
    x(i)=ligne(1);
    y(i)=ligne(2);
    z(i)=ligne(3);
end;
for i=1:nf
    ligne=fscanf(fid,'%g',4);
    NN(1,i)=ligne(1);
    NN(2,i)=ligne(2);
    NN(3,i)=ligne(3);
    NN(4,i)=ligne(4);
end;
nftri=0;
for i=1:nf
    nftri=nftri+1;
    tri(nftri,:)=[NN(1,i) NN(2,i) NN(3,i)];
    nftri=nftri+1;
    tri(nftri,:)=[NN(1,i) NN(3,i) NN(4,i)];
```

```
    end;
    ligne=fgetl(fid);
    ligne=fgetl(fid);
    for i=1:nf
111     ligne=fscanf(fid,'%g %g',6);
        xu(i)=ligne(1);
        yv(i)=ligne(2);
        zw(i)=ligne(3);
        u(i)=ligne(4);
116     v(i)=ligne(5);
        w(i)=ligne(6);
    end;
    status=fclose(fid);
    figure;
121 trimesh(tri,x,y,z);
    hold on;
    quiver3(xu,yv,zw,u,v,w);
    title('Mesh for Nemoh');
    clear KH;
126 KH=zeros(6,6);
    fid=fopen([nomrep,filesep,'mesh',filesep,'KH.dat'],'r');
    for i=1:6
        ligne=fscanf(fid,'%g %g',6);
        KH(i,:)=ligne;
131 end;
    status=fclose(fid);
    clear XB YB ZB Mass WPA Inertia
    Inertia=zeros(6,6);
    fid=fopen([nomrep,filesep,'mesh',filesep,'Hydrostatics.dat'],'r');
136 ligne=fscanf(fid,'%s',2);
    XB=fscanf(fid,'%f',1);
    ligne=fgetl(fid);
    ligne=fscanf(fid,'%s',2);
    YB=fscanf(fid,'%f',1);
141 ligne=fgetl(fid);
    ligne=fscanf(fid,'%s',2);
    ZB=fscanf(fid,'%f',1);
```

```
    ligne=fgetl(fid);
    ligne=fscanf(fid,'%s',2);
146 Mass=fscanf(fid,'%f',1)*1025.;
    ligne=fgetl(fid);
    ligne=fscanf(fid,'%s',2);
    WPA=fscanf(fid,'%f',1);
    status=fclose(fid);
151 clear ligne
    fid=fopen([nomrep,filesep,'mesh',filesep,'Inertia_hull.dat'],'r');
    for i=1:3
        ligne=fscanf(fid,'%g %g',3);
        Inertia(i+3,4:6)=ligne;
156 end;
    Inertia(1,1)=Mass;
    Inertia(2,2)=Mass;
    Inertia(3,3)=Mass;
    % Write Nemoh input file
161 fid=fopen([nomrep,filesep,'Nemoh.cal'],'w');
    fprintf(fid,'--- Environment ------------------------------------------------------------------------
    fprintf(fid,'%f                         ! RHO                   ! KG/M**3       ! Fluid specific volu
    fprintf(fid,'%f                         ! G                     ! M/S**2        ! Gravity \n',g);
    fprintf(fid,'0.                 ! DEPTH                 ! M             ! Water depth\n');
166 fprintf(fid,'0. 0.              ! XEFF YEFF             ! M             ! Wave measurement point\n');
    fprintf(fid,'--- Description of floating bodies ---------------------------------------------------
    fprintf(fid,'1                          ! Number of bodies\n');
    fprintf(fid,'--- Body 1 -----------------------------------------------------------------------------
    if isunix
171     fprintf(fid,['''',nomrep,filesep,'mesh',filesep,'axisym.dat''               ! Name of mesh file\n
    else
        fprintf(fid,[nomrep,'\\mesh\\axisym.dat      ! Name of mesh file\n']);
    end;
    fprintf(fid,'%g %g                      ! Number of points and number of panels         \n',nx,nf);
176 fprintf(fid,'6                          ! Number of degrees of freedom\n');
    fprintf(fid,'1 1. 0.    0. 0. 0. 0.             ! Surge\n');
    fprintf(fid,'1 0. 1.    0. 0. 0. 0.             ! Sway\n');
    fprintf(fid,'1 0. 0. 1. 0. 0. 0.                ! Heave\n');
    fprintf(fid,'2 1. 0. 0. 0. 0. %f                ! Roll about a point\n',zG);
```

```
fprintf(fid,'2 0. 1. 0. 0. 0. %f               ! Pitch about a point\n',zG);
fprintf(fid,'2 0. 0. 1. 0. 0. %f               ! Yaw about a point\n',zG);
fprintf(fid,'6                          ! Number of resulting generalised forces\n');
fprintf(fid,'1 1. 0.    0. 0. 0. 0.            ! Force in x direction\n');
fprintf(fid,'1 0. 1.    0. 0. 0. 0.            ! Force in y direction\n');
fprintf(fid,'1 0. 0. 1. 0. 0. 0.               ! Force in z direction\n');
fprintf(fid,'2 1. 0. 0. 0. 0. %f               ! Moment force in x direction about a point\n',zG);
fprintf(fid,'2 0. 1. 0. 0. 0. %f               ! Moment force in y direction about a point\n',zG);
fprintf(fid,'2 0. 0. 1. 0. 0. %f               ! Moment force in z direction about a point\n',zG);
fprintf(fid,'0                          ! Number of lines of additional information \n');
fprintf(fid,'--- Load cases to be solved ------------------------------------------------------------
fprintf(fid,'1  0.8     0.8             ! Number of wave frequencies, Min, and Max (rad/s)\n');
fprintf(fid,'1  0.      0.              ! Number of wave directions, Min and Max (degrees)\n');
fprintf(fid,'--- Post processing -----------------------------------------------------------------
fprintf(fid,'1  0.1     10.             ! IRF                           ! IRF calculation (0 for no cal
fprintf(fid,'0                          ! Show pressure\n');
fprintf(fid,'0  0.      180.            ! Kochin function               ! Number of directions of calcu
fprintf(fid,'0  50      400.    400.    ! Free surface elevation        ! Number of points in x directi
fprintf(fid,'---')
status=fclose(fid);
fclose('all');
end
```

B

APPENDIX B - WEC-SIM INPUT FILE - IRREGULAR WAVES

```
%% Simulation Data
simu = simulationClass();               % Initialize Simulation Class
simu.simMechanicsFile = 'CaseStudy.slx';% Specify Simulink Model File
simu.mode = 'normal';                   % Specify Simulation Mode ('normal','accelerator','rapid-acce
simu.explorer='off';                    % Turn SimMechanics Explorer (on/off)
simu.startTime = 0;                     % Simulation Start Time [s]
simu.rampTime = 100;                    % Wave Ramp Time [s]
simu.endTime=400;                       % Simulation End Time [s]
simu.solver = 'ode4';                   % simu.solver = 'ode4' for fixed step & simu.solver = 'ode45'
simu.dt = 0.1;                                          % Simulation time-step [s]

% Irregular Waves using PM Spectrum
waves = waveClass('irregular');         % Initialize Wave Class and Specify Type
waves.H = 4.78;                         % Significant Wave Height [m]
waves.T = 10.82;                        % Peak Period [s]
waves.waveDir = 280.72;                 % Direction [degrees]
waves.spectrumType = 'PM';              % Specify Wave Spectrum Type

%% Body Data
% Float
body(1) = bodyClass('NEMOH/NEMOH_results.h5');
    %Create the body(1) Variable, Set Location of Hydrodynamic Data File
    %and Body Number Within this File.
body(1).geometryFile = 'geometry/float.stl';
body(1).mass = 'equilibrium';
    %Body Mass. The 'equilibrium' Option Sets it to the Displaced Water
    %Weight.
body(1).momOfInertia = [20907301 21306090.66 37085481.11];  %Moment of Inertia [kg*m^2]

% Translational PTO
pto(1) = ptoClass('PTO1');                      % Initialize PTO Class for PTO1
pto(1).k = 0;                                   % PTO Stiffness [N/m]
```

```
33  pto(1).c = 1200000;                    % PTO Damping [N/(m/s)]
    pto(1).loc = [0 0 0];                  % PTO Location [m]
```